(12) INTERNATIONAL APPLICATION PUBLISHED UNDER THE PATENT COOPERATION TREATY (PCT)

(19) **World Intellectual Property Organization**
International Bureau

(43) **International Publication Date**
27 January 2022 (27.01.2022)

WIPO | PCT

(10) **International Publication Number**
WO 2022/019840 A1

(51) **International Patent Classification:**
H01Q 5/35 (2015.01) *H01Q 1/38* (2006.01)
H01P 1/161 (2006.01) *B33Y 80/00* (2006.01)
G06N 3/00 (2006.01) *H01P 3/127* (2006.01)
H01Q 13/02 (2006.01) *H01P 3/123* (2006.01)
H01Q 15/00 (2006.01) *H01P 11/00* (2006.01)

(21) **International Application Number:**
PCT/SG2021/050430

(22) **International Filing Date:**
22 July 2021 (22.07.2021)

(25) **Filing Language:** English

(26) **Publication Language:** English

(30) **Priority Data:**
10202007125R 24 July 2020 (24.07.2020) SG

(71) **Applicant: NATIONAL UNIVERSITY OF SINGAPORE** [SG/SG]; 21 Lower Kent Ridge Road, Singapore 119077 (SG).

(72) **Inventors: GUO, Yongxin**; c/o National University of Singapore, Faculty of Engineering, Department of Electrical and Computer Engineering, 21 Lower Kent Ridge Road, Singapore 119077 (SG). **MA, Boyuan**; c/o National University of Singapore, Faculty of Engineering, Department of Electrical and Computer Engineering, 21 Lower Kent Ridge Road, Singapore 119077 (SG). **WU, Jie**; c/o National University of Singapore, Faculty of Engineering, Department of Electrical and Computer Engineering, 21 Lower Kent Ridge Road, Singapore 119077 (SG). **LI, Xun**; c/o National University of Singapore, Faculty of Engineering, Department of Electrical and Computer Engineering, 21 Lower Kent Ridge Road, Singapore 119077 (SG). **WANG, Cong**; c/o National University of Singapore, Faculty of Engineering, Department of Electrical and Computer Engineering, 21 Lower Kent Ridge Road, Singapore 119077 (SG).

(74) **Agent: DAVIES COLLISON CAVE ASIA PTE. LTD.**; 10 Collyer Quay #07-01, Ocean Financial Centre, Singapore 049315 (SG).

(81) **Designated States** *(unless otherwise indicated, for every kind of national protection available)*: AE, AG, AL, AM, AO, AT, AU, AZ, BA, BB, BG, BH, BN, BR, BW, BY, BZ, CA, CH, CL, CN, CO, CR, CU, CZ, DE, DJ, DK, DM, DO, DZ, EC, EE, EG, ES, FI, GB, GD, GE, GH, GM, GT, HN, HR, HU, ID, IL, IN, IR, IS, IT, JO, JP, KE, KG, KH, KN, KP, KR, KW, KZ, LA, LC, LK, LR, LS, LU, LY, MA, MD, ME, MG, MK, MN, MW, MX, MY, MZ, NA, NG, NI, NO, NZ, OM, PA, PE, PG, PH, PL, PT, QA, RO, RS, RU, RW, SA, SC, SD, SE, SG, SK, SL, ST, SV, SY, TH, TJ, TM, TN, TR, TT, TZ, UA, UG, US, UZ, VC, VN, WS, ZA, ZM, ZW.

(84) **Designated States** *(unless otherwise indicated, for every kind of regional protection available)*: ARIPO (BW, GH, GM, KE, LR, LS, MW, MZ, NA, RW, SD, SL, ST, SZ, TZ, UG, ZM, ZW), Eurasian (AM, AZ, BY, KG, KZ, RU, TJ, TM), European (AL, AT, BE, BG, CH, CY, CZ, DE, DK, EE, ES, FI, FR, GB, GR, HR, HU, IE, IS, IT, LT, LU, LV, MC, MK, MT, NL, NO, PL, PT, RO, RS, SE, SI, SK, SM,

(54) **Title:** UNITARY HORN ANTENNA

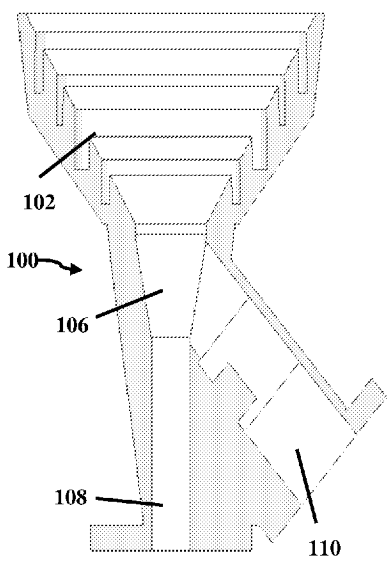

Figure 4(c)

(57) **Abstract:** A unitary device comprising a horn antenna disposed about a horn axis and having an engineered inner surface; and an integrated orthomode transducer comprising a waveguide transition and at least two separate waveguides each having an internal surface, the waveguide transition connecting the at least two separate waveguides to the antenna, wherein the orthogonal transducer is adapted to couple at least two orthogonal linear polarized fields from the at least two separate waveguides into the waveguide transition for transmission by the antenna, and/or decouple at least two orthogonal linear polarized fields received by the waveguide transition from the antenna into respective ones of the at least two separate waveguides.

WO 2022/019840 A1

[Continued on next page]

TR), OAPI (BF, BJ, CF, CG, CI, CM, GA, GN, GQ, GW, KM, ML, MR, NE, SN, TD, TG).

Declarations under Rule 4.17:
— *of inventorship (Rule 4.17(iv))*

Published:
— *with international search report (Art. 21(3))*
— *in black and white; the international application as filed contained color or greyscale and is available for download from PATENTSCOPE*

Unitary Horn Antenna

Technical Field

The present invention relates, in general terms, to a unitary horn antenna, and also relates to methods of manufacturing and designing the horn antenna.

Background

In satellite communications, reflector antennas are prevalent for their ease of fabrication and reliability. To obtain flexible operating bands, high gain, and beam equalization, corrugated horns are preferred as the feed antenna. As for the fabrication process, the manufacture of common horn antennas and their feeding structures is through machine tools. Since integrated fabrication is hardly feasible, assembly and fixing are necessary. Alignment and stability are guaranteed through flanges with screw holes, which results in a bulky size. Simple horn antennas are carved out of a metallic puck through a milling machine. If the internal wall has an intricate pattern, the inner and outer parts of the horn are fabricated separately. When the configuration becomes more complex, the antenna is halved into two parts.

Traditional methods based on machine tools are divided into three types: a) the horn is directly carved out of a metallic puck through a milling machine, as seen in Figure 1(a). This method applies to simple structures. It is reliable due to mature machining technology. However, during the milling process, considerable material is wasted. b) If the internal wall has an intricate pattern, the inner and outer parts of the horn are fabricated separately, as seen in Figure 1(b). Consequently, the assembly process is complicated. The stability of the structure is also questionable. c) When the structure becomes more complex, the horn is halved into two identical parts from the symmetrical plane to facilitate fabrication, as seen in Figure 1(c). The two parts are then aligned and fixed together through flanges with screw holes. This approach wastes lots of material for alignment and assembly. It has a bulky size, large weight, and stability problems. As for OMTs, the fabrication process is similar to the method c) for horns shown in Figure 1(c).

The corrugated horn and OMT could be devised by analytical methods. But for compact and irregular configurations, a more versatile approach is iterative optimization with initial values derived by theory and experience. Optimizer-based design methods gain increasing attention in electronic engineering. Recently, a novel nature-inspired algorithm, the grey wolf optimizer (GWO), was introduced to antenna design and array synthesis. Due to its concise framework and excellent performance, the GWO has been adopted in diverse fields. However, for electromagnetic design problems, studies in this optimizer are insufficient. Exclusive modifications on the GWO are demanded to reduce simulation cost and accelerate convergence.

It would be desirable to overcome or at least one of the above-described problems, or at least to provide a useful alternative.

Summary

Disclosed herein is a unitary device comprising a horn antenna disposed about a horn axis and having an engineered inner surface; and an integrated orthomode transducer comprising a waveguide transition and at least two separate waveguides each having an internal surface, the waveguide transition connecting the at least two separate waveguides to the antenna, wherein the orthogonal transducer is adapted to couple at least two orthogonal linear polarized fields from the at least two separate waveguides into the waveguide transition for transmission by the antenna, and/or decouple at least two orthogonal linear polarized fields received by the waveguide transition from the antenna into respective ones of the at least two separate waveguides.

In some embodiments, the inner surface of the horn antenna is designed according to a broad class of optimisation algorithms.

In some embodiments, the internal surface of at least one of the at least two separate waveguides is designed according to a broad class of optimisation algorithms.

In some embodiments, the horn antenna has a circular cross-section.

In some embodiments, the horn antenna has a square cross-section.

In some embodiments, the horn antenna is adapted to support two or more waveguide modes corresponding to the at least two orthogonal linear polarized fields.

In some embodiments, the horn antenna operates in 12.25-12.75 GHz and 14-14.5 GHz.

In some embodiments, the waveguide transition is a quasi-elliptical waveguide transition connecting a rectangular and a circular waveguide.

In some embodiments, the inner surface of the horn antenna comprises a plurality of ridges, each ridge having a horizontal ridge width, being oriented parallel to the horn axis, with the ridge being located at slots along the inner surface of the horn antenna, each slot having a vertical slot height, and a horizontal slot width, being oriented parallel to the horn axis.

In some embodiments, the horn antenna has a flare angle being the angle between a line drawn parallel to the horn axis and a line passing through a top surface of adjacent ones of said ridges.

In some embodiments, the unitary device according is formed from at least one of a metal material and a plastic material.

In some embodiments, the waveguide transition tapers away from the horn antenna.

In some embodiments, the at least one of the at least two of the separate waveguides has a rectangular cross-section.

In some embodiments, the at least one of the at least two of the separate waveguides has a circular cross-section.

In some embodiments, the at least one of the at least two of the separate waveguides has a waveguide axis at a non-zero angle to the horn axis.

In some embodiments, a length of the at least one of the at least two of the separate waveguides is formed from a sequence of sections, each section having a length, width and height, and varying from each adjacent said section in the sequence, in at least one of the length, width and height.

Disclosed herein is an antenna assembly, comprising a unitary device; a perforated reflector; and a platform for stabilizing the utility device and the perforated reflector, wherein the horn antenna of the unitary device functions as the feed for the perforated reflector, and a phase center of the horn antenna of the unitary device is at a focus of the perforated reflector.

Disclosed herein is a manufacturing method for manufacturing the antenna assembly according to 17, comprising manufacturing at least one of the unitary device, the perforated reflector, and the platform using three-dimensional printing technology.

Disclosed herein is a manufacturing method for manufacturing the unitary device according, comprising manufacturing the unitary device in at least two separate blocks.

In some embodiments, the manufacturing method further comprises at least one of manufacturing each part of the at least two separate blocks as one or more of external protrusions, holes and partially holes; and providing alignment pins and threaded holes on the at least two separate blocks to facilitate assembly.

Disclosed herein is a method of designing the horn antenna or the separate waveguides of the orthomode transducer based on grey wolf optimizer, comprising generating initialization population in a pre-defined solution space; calculating a fitness value of each grey wolf in the initialization population according to a pre-defined fitness function, each grey wolf defining a solution at a position in the solution space; and repeatedly: selecting a predetermined number of fitness values based on an ordering of fitness values from large to small ("**best fitness values**"), and identifying and storing as X_α, X_β, and X_δ a position of each best fitness value based on the respective grey wolf; updating and storing position for each grey wolf according to one or more pre-defined functions; and updating and storing the fitness value of each grey wolf in each updated position according to the pre-defined fitness function; and outputting X_α when a predetermined maximum number of repetitions is reached.

In some embodiments, for each repetition of updating a position for each grey wolf, the method further comprises comparing the updated position with each position of a previous repetition, to determine whether or not to update the fitness value with the updated position.

In some embodiments, the fitness function for designing the horn antenna according to any one of 1 to 7 is determined according to:

$$F_{horn} = B_1 f_{S_{11}} + B_2 f_{Beam} + B_3 f_{XP} + B_4 f_{Size}, \text{ where } \sum_n B_n = 1$$

$$f_{S_{11}} = \sum_{m=1}^{2} u(S_{11\_max}(m) + 20)(S_{11\_max}(m) + 20)^2$$

$$f_{Beam} = \sum_{i=1}^{2} (\max_{j=1,2,3} |BW_{12dB}(i,j) - 63|)^2$$

$$f_{XP} = \sum_{i=1}^{2} u(\max_{j=1,2,3} XPL(i,j) + 30)(\max_{j=1,2,3} XPL(i,j) + 30)^2$$

$$f_{Size} = u(\sum_k d_k - d_{total})(\sum_k d_k - d_{total})^2$$

in which B_i (i=14) is the positive weighted coefficient indicating the importance of each requirement, $u(x)$ denotes step function, $S_{11\_max}(m)$ is maximum S_{11} parameter in dB in the m-th band, $Bandwidth_{12dB}(i,j)$ and $XPL(i,j)$ are the 12dB beamwidth in degree and cross-polarization level in dB, respectively, in the j-th plane at the i-th frequency, d_k denotes the horizontal ridge width and the horizontal slot width in mm, and d_{total} is size limitation of the horizontal ridge width and the horizontal slot width.

In some embodiments, the fitness function for designing the horn antenna according to any one of 1 to 7 is determined according to:

$$F_{OMT} = D(\sum_n c_n - c_{total})^2 u(\sum_n c_n - c_{total}) + (1-D)(S_{11max} + 20)^2 u(S_{11max} + 20)$$

in which D denotes a positive weighted coefficient, $u(x)$ denotes step function, $S_{11\_max}(i)$ is maximum S_{11} parameter in dB in the operating band, c_n denotes the horizontal interval width for the n-th interval.

Brief description of the drawings

Embodiments of the present invention will now be described, by way of nonlimiting example, with reference to the drawings in which:

Figure 1(a) shows an example horn that is directly carved out of a metallic puck through a milling machine;

Figure 1(b) shows an example horn where the inner and outer parts are fabricated separately;

Figure 1(c) shows an example horn that is halved into two identical parts from the symmetrical plane to facilitate fabrication;

Figure 2(a) shows an example dielectric horn antenna;

Figure 2(b) and (2c) show an example plastic horn that is halved into two parts;

Figure 3(a) and 3(b) shows an example metallic horn and its OMT;

Figure 4(a) through 4(e) illustrates an example unitary device comprising a horn antenna and an integrated orthomode transducer comprising a waveguide transition and at least two separate waveguides;

Figure 5(a) through(c) shows an example antenna assembly, comprising a unitary device, a perforated reflector, and a platform;

Figure 6 illustrates an example optimization process for designing the corrugated horn antenna or the separate waveguides of the orthomode transducer based on grey wolf optimizer;

Figure 7 illustrates an optimization result using the optimization process in Figure 5;

Figure 8(a) through(e) show the performance of the horn of Figure 5;

Figure 9 illustrates the comparison between the original and modified encircling coefficients;

Figure 10 illustrates an example optimization process for designing the corrugated horn antenna or the separate waveguides of the orthomode transducer based on grey wolf optimizer;

Figure 11 shows the comparison between GWO and MGWO based on Opt II in Table IV;

Figure 12(a) through(d) illustrates optimization results using the optimization process in Figure 10 based on Opt I-IV in Table IV;

Figure 13(a) illustrates comparison between GWO and MGWO based on Opt II in Table IV regarding average achievable cost value after each iteration;

Figure 13(b) illustrates comparison between GWO and MGWO based on Opt II in Table IV regarding average required iteration to achieve certain cost value;

Figure 14(a) and(b) illustrate fabricated integrated dual-band design horn antenna H1 and wideband design antenna H2 with adaptors, respectively;

Figure 15(a) and(b) illustrate simulated and measured S parameters for dual-band antenna H1 and wideband antenna H2, respectively; and

Figure 15(a) through(d) illustrates simulated and measured radiated patterns for E-plane pattern at 12.5 GHz, H-plane pattern at 12.5 GHz, E-plane pattern at 14.25 GHz, H-plane pattern at 14.25 GHz.

Detailed description

The present disclosure relates to a unitary device comprising a compact light-weighted dual-band dual-polarized horn antenna. The horn is adapted to work with two orthogonal polarizations for receiving and transmitting, respectively. The proposed antenna functions as a feed horn of a reflector for Ku-band satellite communications. It will be appreciated that the antenna could work in dual bands, for example 12.25-12.75 GHz and 14-14.5 GHz. The proposed antenna is a dual-polarized antenna horn with an integrated orthomode transducer orthomode transducer (OMT) presented for satellite communications. The proposed OMT is applied as the feeding structure, and is with a tilted branch which is integrated below the horn so that separate fabrication and redundant structures are not needed. The integrated structure increases its versatility and reliability in severe scenarios.

The proposed unitary device comprises an automatically designed all-integrated three-dimensional (3D)-printed horn antenna. The configuration of the antenna structure is compatible with direct 3D metal printing technology. An integrated antenna structure suitable for direct printing is devised and validated. Material waste caused by the auxiliary supports during printing is minimized. Assembly, aligning, and fixtures are also unnecessary, resulting in compactness. Such an antenna, albeit as an all-metal structure, has a light weight of 200 g. It will be appreciated that this integrated antenna can be readily fabricated through a 3D printer all in once. A corrugated horn can be adopted as the aperture antenna. This type of horn is broadly used for its excellent beam equalization in E-, H-, and diagonal planes, and a steady phase center.

Unless context dictates otherwise, as used herein the term “unitary” refers to the device being fabricated as a single component or item. For example, A “unitary device” will comprise the horn antenna and integrated OMT formed together as a single component or item.

Such a unitary device (100) is shown in Figure 4. Broadly, the unitary device 100 comprises:

a horn antenna (102) disposed about a horn axis and having an engineered inner surface; and

an integrated OMT comprising a waveguide transition (106) and at least two separate waveguides (108 and 110) each having an internal surface, the waveguide transition 106 connecting the at least two separate waveguides 108 and 110 to the antenna 102, wherein the OMT 104 is adapted to couple at least two orthogonal linear polarized fields from the at least two separate waveguides into the waveguide transition for transmission by the antenna 102, and/or decouple at least two orthogonal linear polarized fields received by the waveguide transition from the antenna 102 into respective ones of the at least two separate waveguides 108 and 110.

Figure 4(d) illustrates the structure of the horn 102. The corrugated horn 102 with four vertical slots (112) is chosen (see Figure 4(d)). In particular, the inner surface of the horn antenna 102 comprises a plurality of ridges (114) (see Figure 2(d)), each ridge having a horizontal ridge width (i.e., d_1, d_3, d_5, and d_7), being oriented parallel to the horn axis, with the ridge being located at slots 112 along the inner surface of the horn antenna, each slot having a vertical slot height (i.e., l_1, l_2 l_3, and l_4), and a horizontal slot width (i.e., d_2, d_4, d_6, and d_8), being oriented parallel to the horn axis. The horn antenna 102 also has a flare angle (i.e., φ_h) being the angle between a line drawn parallel to the horn axis and a line passing through a top surface of adjacent ones of said ridges 114.

The OMT consists of a tapering transition 106, a direct branch 108, and a tilted one 110. The waveguide transition 106 is a quasi-elliptical waveguide transition connecting a rectangular (i.e., 108) and a circular waveguide (i.e., 110). In some embodiments, said 106 is designed to taper away from the horn antenna 102. In some embodiments, the at least one of 108 and 110 has a circular cross-section. In some other embodiments, the at least one of 108 and 110 has a rectangular cross-section. Said titled branch 110 has a waveguide axis at a non-zero angle to the horn axis (see Figure 4(e)).

It will be appreciated that said tilted branch 110 may be formed from a sequence of sections (116), each section having a length (i.e., a_1, a_2, a_3, and a_4), width (i.e., b_1, b_2, b_3, and b_4) and height (i.e., c_1, c_2, c_3, and c_4), and varying from each adjacent said section in the sequence, in at least one of the length, width and height. In one embodiment, the tilted one 110 adopts a four-step configuration (see Figure 4(b)) for impedance matching. The performance of the horn and OMT hardly influences each other so that they are optimized independently as illustrated in Figure 4(c). As will be discussed in details, the inner surface of the horn antenna 102 is designed according to a broad class of optimization algorithms, which will discussed in full details. Also, the internal surface of at least one of the at least two separate waveguides is designed according to a broad class of optimization algorithms.

In Ku-band satellite communications, reflectors antennas such as the device 100 with the feed horn 102 are prevalent for their flexible bandwidth, ease of fabrication, and reliability. To obtain the required bandwidth and excellent beam equalization, a corrugated horn with various types of cross-sections and slots is preferred. In some embodiments, the horn 102 has a circular cross-section. In some other embodiments, the horn has a square cross-section. It will be appreciated that the disclosure herein may be made generally with reference to horn antennae having a corrugated inner surface. However, it will be appreciated that other engineered inner surfaces may be used – e.g. flat, undulating, slotted, grooved, paraboloid, hyperboloid, spheroid and any other inner surface shape or arrangement necessary to achieve a particular and desired purpose.

In some embodiments, the horn antenna is adapted to support two or more waveguide modes corresponding to the at least two orthogonal linear polarized fields. In the present disclosure, the horn antenna operates in 12.25-12.75 GHz and 14-14.5 GHz. The horn antenna 102 may work with two orthogonal linear polarizations for receiving and transmitting modes, respectively. Accordingly, the OMT is widely applied as the feeding structure. The design of the corrugated horn 102 and its OMT could base on analytical analysis in limited cases. As will be discussed in more details, a more versatile method is to conduct iterative optimization in light of the performance requirement. For compact designs where a short corrugated horn only has 3-4 slots and its OMT is irregular, a powerful optimizer is highly required. The designer may set the initial configuration of the antenna according to analytical and empirical equations, or directly launch the optimizer with random initial values. This design process is automated, which significantly saves time and human costs.

Figure 5(b) shows an example antenna assembly (500), comprising the unitary device 100, a perforated reflector (502), and a platform (504). The device 100 here is equipped on the platform 504 with the help of a choking fixture (506) and a pad (508) below. The platform 504 is used for stabilizing the utility device 100 and the perforated reflector 502. In one example as shown in Figure 5(b), the horn antenna of the unitary device functions as the feed for the perforated reflector 502. As illustrated in Figure 5(c), the device 100 has an angle (i.e., θ_0) being the angle between a line drawn parallel to the platform axis and a line passing through the centre of the reflector 502. Said angle θ_0 is set such that a phase centre of the horn antenna 102 of the unitary device 100 is at a focus of the perforated reflector 502.

The design of the antenna configuration in the present disclosure follows two principles. The first principle is that the structure needs to be compatible with direct 3D printing, where assembly is not required. All suspended part should have a tilted angle of no more than 45° so that it does not collapse during fabrication. Said 3D printing is a potential candidate to substitute the traditional machining process in horn antenna manufacturing. The size and weight of the antenna 102 can be significantly reduced, which saves much fabrication time and cost. In particular, two types of techniques can be applied—plastic and metal 3D printing. For plastic printing, a dielectric horn antenna is printed first (Figure 2(a)). Then, electroplating, conductive spray paint, or metal coating is conducted to achieve metallization. Apparently, for inner walls of horn antennas, this is inconvenient. Hence, the plastic horn is always halved into two parts, as seen in Figure 2(b) and Figure 2(c). The whole fabrication process consists of printing, metallization, and assembly.

Another possible 3D printing method is based on metallic material, especially the aluminium alloy $AlSi_{10}Mg$. The horn antenna is directly printed layer by layer through additive manufacturing. Nevertheless, the structure for metal printing cannot be arbitrary. Suspended stubs longer than several millimetres are usually not feasible unless redundant support is used. Likely, the tilted angle of the structure should not exceed 45° to avoid collapsing due to gravity. Therefore, the metallic horn and its OMT are printed separately to increase design freedom. Flanges with screw holes are needed for fixing, which increases the antenna volume and impairs its stability and sealing performance. In some examples, the antenna assembly 500 as a whole can be manufactured using 3D printing technology. It will be appreciated that in some embodiments, the antenna assembly 500 especially the unitary device 100 according is formed from at least one of a metal material and a plastic material. The unitary device and/or assembly may be manufactured in at least two separate block. In one embodiment, the unitary device is manufactured by manufacturing the antenna 102 and OMT separately. In another embodiment, the unitary device 100 is manufactured by manufacturing the antenna 102, the waveguide transition 106 and the waveguides 108 and 110 separately. It will be appreciated that alignments pins and threaded holes can be provided on the separate blocks to facilitate assembly.

The second principle for the design of the antenna configuration is that the configuration needs to be easy to optimize, which means that the dimension of the solution space should be minimized. In the present disclosure, according to the proposed antenna configuration, an optimization problem is constructed to design the antenna automatically based on Matlab-HFSS co-simulation. The impedance matching, radiation pattern, cross-polarization level (XPL), and antenna size are considered. The antenna 102 is designed as the feed of a reflector for Ku-band satellite communications. Therefore, the operating band, gain, cross-polarization level (XPL), and beamwidth in E-, H-, and diagonal planes need optimization. Besides, the size of the antenna is optimized as well for compactness. Since the antenna is divided into the radiation and feeding parts shown in Figure 4(c)-(e), the optimization problem is decomposed into two sub-problems, i.e., OptHorn and OptOMT, respectively. Parallel optimization is thus feasible. Meanwhile, the dimension of the solution space is greatly reduced. The variables for optimization are illustrated in Figure 4(d) and(e). The performance requirements for each part are listed in Table I.

Table I

PERFORMANCE REQUIREMENT

	Horn	OMT
Operating band (GHz)	12.25-12.75, 14-14.5	Port1: 12.25-12.75, Port2: 14-14.5
Gain (dBi)	>16	--
XP level (dB)	<-25	--
12 dB Beamwidth in E-, H-, and diagonal planes (deg)	63	--

The proposed automated design process bases on a modified GWO which will be demonstrated later. The original GWO is a single-objective algorithm. Its multi-objective versions were proposed, which is not necessary in this disclosure. Hence, a fitness function for OptHorn is put forward in (1). It consists of five components representing the wanted radiation behaviors, input characteristics, and antenna size.

$$F_{horn} = B_1 f_{S_{11}} + B_2 f_{Beam} + B_3 f_{XP} + B_4 f_{Size},\ \text{where} \sum_n B_n = 1$$

$$f_{S_{11}} = \sum_{m=1}^{2} u(S_{11\_max}(m) + 20)(S_{11\_max}(m) + 20)^2$$

$$f_{Beam} = \sum_{i=1}^{2} (\max_{j=1,2,3} |BW_{12dB}(i,j) - 63|)^2$$

$$f_{XP} = \sum_{i=1}^{2} u(\max_{j=1,2,3} XPL(i,j) + 30)(\max_{j=1,2,3} XPL(i,j) + 30)^2$$

$$f_{Size} = u(\sum_k d_k - d_{total})(\sum_k d_k - d_{total})^2 \quad (1)$$

in which B_i (i=14) is the positive weighted coefficient indicating the importance of each requirement, $u(x)$ denotes step function, $S_{11\_max}(m)$ is maximum S_{11} parameter in dB in the m-th band, $Bandwidth_{12dB}(i,j)$ and $XPL(i,j)$ are the 12dB beamwidth in degree and cross-polarization level in dB, respectively, in the j-th plane at the i-th frequency, d_k denotes the horizontal ridge width and the horizontal slot width in mm, and d_{total} is size limitation of the horizontal ridge width and the horizontal slot width.(d)

Similarly, the fitness function of OptOMT is set as:

$$F_{OMT} = D(\sum_n c_n - c_{total})^2 u(\sum_n c_n - c_{total}) + (1 - D)(S_{11\max} + 20)^2 u(S_{11\max} + 20) \quad (2)$$

where D is a positive weighted coefficient, $u(x)$ is the step function, S_{11max} is the maximum S_{11} parameter in dB in the operating band, c_k is the OMT parameter in mm shown in Figure 4(e), and c_{total} represents the size limitation of the OMT. The two sub-problems are summarized in Table II.

Table II

OPTIMIZATION SUBPROBLEMS

	OptHorn	OptOMT
Variables	Slot and tooth width d_k (mm), k=1~9; Slot depth l_m (mm), m=1,2,3,4;	Step width a_n (mm), step height b_n (mm), and step length c_n (mm), n=1~4; Start point of the tilted branch c_0 (mm).

	Flare angle of the horn φ_h (deg).	
Dimension	14	13
Fitness function	Eq.(1)	Eq.(2)

In the present disclosure, an algorithm-based design method is proposed for said Ku-band satellite communications. The whole structure of the proposed horn antenna is automatically designed through a swarm intelligence-based algorithm, i.e., the GWO, to obtain fine antenna performance and compact size. The GWO was proposed in 2014. With a concise framework, it shows competitive or even superior performance when compared with classical global optimization algorithms, such as the genetic algorithm, particle swarm optimization, differential evolution, etc. It has been proved that this optimizer has great potential in electromagnetics. A compact antenna structure is put forward, of which the design process is decomposed into two sub-problems to accelerate optimization. The original GWO is modified exclusively for electromagnetic design problems so that the time cost is reduced. It will be appreciated that said automated design and fabrication approaches are proposed based on both modified GWO and 3D metal printing. To make the algorithm compatible with the 3D printing process, some novel application-based modifications can be added to the algorithm. Through the proposed design method, time, human, and material costs are decreased. In particular, the manufacturing time and cost are thus considerably reduced compared to those of existing designs based on machining and separate printing. The proposed design particularly applies to design automation and mass production. Fine agreement is observed between the simulated and measured results, showing the superiority of the proposed integral design and fabrication process.

Since the GWO has been evaluated and compared with other classical algorithms in the prior art in a comprehensive manner, the present invention directly uses a practical design problem to demonstrate the performance of the algorithm. Some application-oriented modifications are added to the original GWO.

According to the machining error of 3D metal printing, hypersensitive solutions are not feasible. Therefore, a filter is inserted into the GWO code to eliminate these solutions. The machining error of the available 3D printing technology is also under consideration. The step of the solution searching process is rectified. Moreover, an extra stop criterion is added so that the GWO can stop in advance to save the time cost of the design. The optimization process of the OMT shown in Figure 4(e) and Table III is visualized in Figure 6. as an instance. It is observed that with a sample amount comparable to the dimension of the solution space in each iteration, the GWO shows excellent performance, which coincides with the result. After 22 iterations, the maximal S11 parameter obtained by the GWO already reaches -15 dB in the two bands. At the last iteration, the value is further optimized to -20 dB. Since the optimization processes of the horn and OMT are in parallel, the overall design time can be reduced to one day.

Figure 6 illustrates an example optimization method 600 for designing the corrugated horn antenna or the separate waveguides of the orthomode transducer based on GWO. Broadly, the method 600 comprises:

Step 602: generating initialization population in a pre-defined solution space;

Step 604: calculating a fitness value of each grey wolf in the initialization population according to a pre-defined fitness function, each grey wolf defining a solution at a position in the solution space; and

Step 606: repeatedly:

selecting a predetermined number of fitness values based on an ordering of fitness values from large to small ("**best fitness values**"), and identifying and storing as X_α, X_β, and X_δ a position of each best fitness value based on the respective grey wolf;

updating and storing position for each grey wolf according to one or more pre-defined functions; and

updating and storing the fitness value of each grey wolf in each updated position according to the pre-defined fitness function; and

Step 608: outputting X_α when a predetermined maximum number of repetitions is reached.

This GWO algorithm is inspired by the social hierarchy and group hunting mechanism of grey wolves. In some embodiments, for each repetition of updating a position for each grey wolf, the method further comprises comparing the updated position with each position of a previous repetition, to determine whether or not to update the fitness value with the updated position. This algorithm showed supreme performance in nonlinear and nonconvex continuous-value problems with a high-dimensional solution space. It has also been evaluated and compared with other classical algorithms in a comprehensive manner. To explain the design process, an example is presented in Table III. The integrated antenna is divided into two parts, the horn and OMT, as seen in Figure 4(c). This simplifies the optimization problem by dividing it into two sub-problems and reducing the dimension of the solution space. The variables for optimization are illustrated in Figure 4(d) and(e), and Table I. The antenna is optimized to have compact size and required performance, in terms of beam widths in E-, H-, and diagonal planes; and voltage standing wave ratio (VSWR) or reflection coefficient. The optimization starts with a set of random initial variables. The goal of the algorithms in Figure 6 is to minimize the value of the objective functions in Table III.

Table III

The optimization process of the integrated antenna through GWO

	Corrugated horn	Tilted OMT branch
Variables for optimization	Width w_i, depth l_i, and location d_i of each slot, i=1,2,3,4; Flare angle of the horn ang_{horn}, Aperture length d	Width a_j, height b_j, and length c_j of each step, j=1,2,3,4; Start point of the tilted branch z

Dimension of the solution space	14	13
Wolf population	20	15
Max iteration	54	54
Objective Function (***A*** and ***B*** are designer-defined positive constants)		
Corrugated horn	$A(\lvert Beamwidth_{12dB}(\text{deg})-63\rvert)\Big\rvert_{\text{frequencies}}^{\text{at two}}\Big\rvert_{planes}^{\text{in } three}+\max(VSWR)\Big\rvert_{\text{bands}}^{\text{in dual}}+\sum_{i=1}^{4}(w_i+d_i)$	
Tilted OMT branch	$\max(S_{11}(dB)\Big\rvert_{bands}^{\text{in } dual})$	

Though the GWO has a concise mechanism, low memory requirement, and excellent performance, according to the no free lunch theorem, exclusive modifications still conduce to improving its performance in actual applications. Therefore, a modified GWO (MGWO) is proposed in the present invention for electromagnetic (EM) automated design in light of the principles below.

a) The running time of the algorithm is trivial compared to full-wave simulation.
b) Excessive simulation runs for a global optimum are not be required all the time. Feasible solutions are acceptable.
c) Hypersensitive solutions are not preferred due to the lack of robustness against manufacturing and simulation errors.
d) The balance between the exploration and exploitation abilities of the optimizer is maintained.
e) Extra tuning parameters are unfavorable.

In the present disclosure, said MGWO with reduced hunting expanse, enhanced solution robustness, an adaptive step size, sample filtering, and re-initialization is proposed to automate and shorten the design process. The whole structure is divided into two independent parts to simplify the optimization problem. The performance and size of the antenna are simultaneously optimized. Moreover, the configuration of the antenna is highly compatible with direct 3D printing technology so that separate fabrication is not needed. Redundant aligning, supporting, or fixing structures are also eliminated as much as possible for compactness. At last, for validation, a 3D-printed all-integrated horn antenna is fabricated and measured. It is then equipped to a reflector.

The GWO mimics the social hierarchy and hunting behavior of grey wolves. It uses the top three historical solutions (alpha, beta, and delta wolves, i.e., the top three historical solutions) to estimate the position of the temporary optimum and guide the searching behavior and to lead the wolf group to search for the prey (optimum). The operator for variable updating is referred to as "encircling". The searching behavior is depicted by

$$\mathbf{x}(t+1) = \mathbf{x}_P(t) - \mathbf{A}\left|\mathbf{C}\mathbf{x}_P(t) - \mathbf{x}(t)\right| \tag{3}$$

where $\mathbf{x}(t+1)$ and $\mathbf{x}(t)$ are the position vectors of one wolf in $(t+1)$-th and t-th iterations, $\mathbf{x}_P(t)$ is the assumed optimum, and **A** and **C** are two diagonal matrices defined as:

$$\mathbf{A} = (2\mathbf{R}_1 - \mathbf{I})a \tag{4}$$

$$\mathbf{C} = 2\mathbf{R}_2 \tag{5}$$

where $\mathbf{R}_1$ and $\mathbf{R}_2$ are two diagonal matrices of which elements have random values between [0, 1], **I** is the identity matrix, and a is called the encircling coefficient formulated by:

$$a = 2(1 - \frac{t}{T}) \tag{6}$$

where t represents the current iteration number, and T is the total iteration number. An encircling operator, **L**, is then derived from (3)-(6)—

$$\mathbf{x}(t+1) = \mathbf{L}(\mathbf{x}_P, t)\mathbf{x}(t) \tag{7}$$

In the GWO, the position of each wolf is updated according to the best three historical positions (alpha, beta, and delta wolves) through the encircling operator, that is:

$$\mathbf{x}_{\alpha,\beta,\delta}(t+1) = \mathbf{L}(\mathbf{x}_{\alpha,\beta,\delta}, t)\mathbf{x}_{\alpha,\beta,\delta}(t)$$

$$\mathbf{x}_i(t+1) = \frac{1}{3}(\mathbf{L}(\mathbf{x}_\alpha, t)\mathbf{x}_i(t) + \mathbf{L}(\mathbf{x}_\beta, t)\mathbf{x}_i(t) + \mathbf{L}(\mathbf{x}_\delta, t)\mathbf{x}_i(t)) \tag{8}$$

where $\mathbf{x}_i(t+1)$ and $\mathbf{x}_i(t)$ are the position vectors of the i^{th} wolf in the $(t+1)^{th}$ and t^{th} iterations, and $\mathbf{x}_{\alpha,\ \beta,\ \delta}$, is the position of the current alpha, beta, and delta wolve, and $\mathbf{x}_i$ is the position vector of the omega wolf.

The original GWO was devised on the basis that simulation cost is trivial since the benchmark functions are in explicit analytical forms. In one single test, tens of independent runs were implemented, each of which had up to 15,000 evaluations. This might be feasible for array synthesis and optimization because only one or none time of full-wave simulation is required. However, for most problems in EM engineering, numerical and full-wave simulations are indispensable in each evaluation. Therefore, a nature-inspired concept, hunting expanse, is introduced to the GWO. It represents the simulation cost during the optimization stage. To reduce hunting expanse, a pack of wolves constructs dynamic collective memory which records the historical positions they have explored. When a wolf is assigned with a new target position, it first compares this position with the existing ones to determine if a new exploration is worthwhile in the next iteration. This is done by:

$$\mathbf{x} = \text{round}(\mathbf{x})$$

$$\text{if } \exists \mathbf{m} \in \mathbf{X}_{memory} \ni \|\mathbf{m} - \mathbf{x}_i(t+1)\|_\infty \le d_{ME}(1 - \frac{t}{T}), \text{ then, } \mathbf{x}_i(t+1) = \mathbf{m} \tag{9}$$

where round($\mathbf{x}$) is the round-off function, $\mathbf{x}$ is a position, vector, $\mathbf{m}$ is a stored position, $\mathbf{X}_{memory}$ is the set of the historical positions that have been actually explored, $\mathbf{x}_i(t+1)$ is the latest position assigned to the i-th wolf, t is the current iteration number, $\|\ \|_\infty$ represents the ∞-norm, T indicates the total iteration number, and d_{ME} is the initial distance threshold determined by the machining error of the available technology. The round-off strategy is based on printing precision. The distance threshold decreases linearly with the iteration number. This forbids solution aggregation during the exploration while preventing optimum missing in the exploitation course. Analogously, the initialization of the GWO is also modified to avoid seed aggregation.

Through Eq.(9), the searching region is discretized, and repetitive searches are forbidden. The hunting expanse thus diminishes. Meanwhile, individual wolves are not encouraged to search for the prey around a poor position, which eliminates the solutions that are hypertensive to fabrication and simulation errors. To further reduce the hunting expanse, an optimization goal is introduced so that the algorithm may stop in advance. The original GWO is designed to minimize the cost function. The only stop criterion is the total iteration number, implying that the optimization goal is minus infinity.

According to Eq.(9), during the exploration stage, if an excellent solution is just a tiny step away from a poor one, it is not adopted due to lack of robustness. Hence, Eq.(9) also eliminates the solutions that are hypertensive to fabrication and simulation errors. This advantage especially applies to 3D-printed horns and OMTs with multiple structural discontinuities. Besides, each element in the positions vector $\mathbf{x}$ is rounded off according to the available manufacture precision from the vendor, which discretizes the solution space for less simulation cost and more robustness.

Besides reducing hunting expanse, another efficient way to cut down the time cost of the GWO-based automated design process is to modify the exploration and exploitation stages simultaneously. It has been proved that when the encircling coefficient a in Eq.(6) is larger than unity, exploration is promoted. In contrast, if $a<1$, exploitation dominates and all wolves start to attack the prey. Several ways have been put forward to amend this coefficient, including adopting nonlinear functions, introducing multiple tuning parameters, using fuzzy logic, etc. However, it has been pointed out that, generally, the encircling coefficient is not correlated to the fitness of each solution. During one group hunting, all individuals update their positions according to the alpha, beta, and delta wolves. Insufficient attention is paid to their own findings, especially when the wolf population is large. This strategy minimizes the memory requirement of the GWO, but as mentioned before, this matters little in EM design. A solution updating approach from an adaptive cuckoo search algorithm is directly adopted, whereas the mechanisms of the two algorithms are different. It is also noticed that in the GWO, the encircling coefficient decreases to zero, suggesting that all but one simulation runs in the last iteration are meaningless. Hence, a novel adaptive encircling coefficient is formulated based on the idea of the dynamic adaption as:

$$a_i(t) = 2(1-\frac{t}{T})^{1+p}, \quad p = r_3\left|\frac{F_{t\_best} - F(\mathbf{x}_i(t))}{F_{t\_best} - F_{t\_worst}}\right|;$$
$$\text{if } t = T, \text{ then } T = T+1. \tag{10}$$

where $a_i(t)$ and $\mathbf{x}_i(t)$ are the encircling coefficient and position vector, respectively, of the i^{th} wolf in the t^{th} iteration, t and T are the current and total iteration numbers, respectively; r_3 is a random value between [0, 1], F_{t_best} and F_{t_worst} are the best and worst fitness values in the t^{th} iteration, and $F(\mathbf{x})$ is the fitness function. The comparison between the original and modified encircling coefficients are shown in Figure 9. In this way, a new searching task is generated partially based on the finding of each individual. Moreover, it is noticed that according to (6), the encircling coefficient decreases to zero in the last iteration. This suggests that the assigned positions might be identical. Hence, a minor modification is introduced to eliminate repetitive simulation. The comparison between the original and modified encircling coefficients is shown in Figure 2(a). For MGWO, the exploration and exploitation behaviors are adaptively adjusted in a dynamic range. Meanwhile, the macroscopic balance between them is well maintained.

At last, the initialization course of the GWO is modified to improve the exploration behavior by avoiding sample aggregation. Normally, the GWO starts with a set of stochastic variables within the solution space, but their even distribution is not well guaranteed. A filtering process similar to (9) is thus inserted after the initialization through:

$$\text{if } \exists \mathbf{x}_i, \mathbf{x}_j \in \mathbf{X}_{initial} \ni \left\| \mathbf{x}_i - \mathbf{x}_j \right\|_2 < \frac{\left\| \mathbf{ub} - \mathbf{lb} \right\|_2}{N_{initial}},$$
$$\text{then, } \mathbf{x}_j \text{ is re-initialized.} \tag{11}$$

where $X_{initial}$ is the initial sample set, $|| \; ||_2$ represents the 2-norm (Euclidean distance), and $N_{initial}$ is the number of initial samples. This filtering operation is conducted N_{dim} times, in which N_{dim} is the dimension of the solution space.

Based on the above approach, an integrated horn antenna that is compatible with metal 3D printing is designed. The design takes a balance between antenna performance and size. No extra procedures, such as assembly, surface processing, alignment, or fixing are needed. Hence, the fabrication time and cost are minimized. Besides, the volume of the antenna is reduced through optimization. The overall height is around $4\lambda_0$ (96 mm), where λ_0 is the wavelength in free space at the center frequency (12.5 GHz) of the lower band. It is light-weighted and more than 30 percent smaller than the compact machining-based horn antenna operating in the same frequency band in the latest publication. Without screws, the mechanical stability of this succinct structure against severe temperature changes and vibration is excellent. These advantages are preferred in portable devices like automotive antennas, and critical systems, such as satellites.

The horn antenna functions as the feed for an offset-fed reflector, as seen in Figure 7. It is equipped on a shared platform seen in Figure 7(b) with the help of a choking fixture and a pad below, as shown in Figure 7(a). The reflector and platform are also implemented through 3D printing. The reflector is densely perforated to reduce the weight of the whole system. The platform stabilizes the antennas and guarantee that the phase center of the feed is at the focus of the reflector. The configuration of the offset-fed reflector antenna is shown in Figure 7(c).

The performance of the antenna is shown in Figure 8. It operates in two separate bands in the Ku band with impressive beam equalization in three vertical sections, as presented in Figure 8(a)-(c). The radiation performance is steady with respect to frequency. After it is equipped to the reflector platform, good radiation behaviors at the two frequencies are still maintained, as shown in Figure 8(d) and (e). Due to the stable phase center of the horn antenna, the aperture efficiency of the reflector is 72.66% and 75.67% at 12.5 GHz and 14.25 GHz, respectively.

Figure 10(a) illustrates an example optimization method 1000 for designing the corrugated horn antenna or the separate waveguides of the orthomode transducer based on MGWO. Broadly, the method 1000 comprises:

Step 1002: generating initialization population in a pre-defined solution space;

Step 1004: calculating a fitness value of each grey wolf in the initialization population according to Eq.(11), each grey wolf defining a solution at a position in the solution space; and

Step 1006: repeatedly:

selecting a predetermined number of fitness values based on an ordering of fitness values from large to small ("**best fitness values**"), and identifying and storing as X_α, X_β, and X_δ a position of each best fitness value based on the respective grey wolf;

updating and storing position for each grey wolf according to Eq.(8), (10) under (9); and

updating and storing the fitness value of each grey wolf in each updated position according to the pre-defined fitness function; and

Step 1008: outputting X_α when a predetermined maximum number of repetitions is reached.

The MGWO does not introduce extra tuning parameters over the original GWO, which makes it application-friendly in various fields. The flow chart of MGWO is shown in Figure 10. To compare the performance of the MGWO and GWO, three different algorithm configurations are adopted for the same optimization problem, as seen in Table III. The goal of the MGWO is set as -20 so that it can stop in advance. The convergence curves are shown in Figure 12(a)-(d). These curves are in line with the features of the GWO, i.e., fast convergence appears in the exploitation stage. Then, OptII was selected for further performance comparison. Ten independent runs were conducted through the GWO and MGWO, respectively. Their average performance is presented in Figure 11. This time, the same stop criterion is applied in the two optimizers. It is observed that the MGWO effectively accelerates the design course.

The GWO and its variants have been tested and compared with other optimizers in terms of tens of algorithm benchmarks. The present disclosure focuses on practical EM design problems since the proposed MGWO is application-oriented. A numerical experiment was conducted, in which the optimization problem of the OMT shown in Figure 1(e) is selected. For comparison, the MGWO, GWO, and genetic algorithm (GA) were applied under the same settings. The S parameter alone was used as the cost function to intuitively demonstrate the performance of the optimizers and eliminate the effect of the weighted coefficient, as seen in Table IV. Four different optimizer configurations were adopted, in which the total simulation runs stayed constant as the population and maximum iteration number varied. The GWO and GA are from Ansys HFSS 2019, respectively. Since the GA has abundant parameters, the default setting was adopted. The optimization goal was set as minimization. To save time, the MGWO was allowed to stop in advance when the cost value is below -20.

Table IV

Problem Configurations	
Dimension	13
Solution vector (mm)	**x** = (c0, a1, a2, a3, a4, b1, b2, b3, b4, c1, c2, c3, c4)
Upper bound (mm)	**ub**=(8, 20, 18, 20, 20, 9, 9, 9, 9, 25, 12, 12, 12)
Lower bound (mm)	**lb** =(0, 5 , 8 , 11, 14, 2, 2, 2 ,2, 10, 2 , 2 , 2)

Cost function	Maximum S11 parameter (dB) in the selected bands, 12.25-12.75 GHz, and 14-14.5 GHz			
Goal	Minimization			
Optimizer Configurations				
Total simulation runs = 600				
	Opt I	Opt II	Opt III	Opt IV
Population	15	20	25	30
Maximum iteration	40	30	24	20

The convergence curves are shown in Figure 12 where a convergence criterion was added during post-processing. The MGWO finds a satisfactory solution after 506.25 simulation runs on average, whereas the GWO requires more than 53 extra runs. Since the population of the three optimizers is identical, the GA fails to converge within the iteration limit. It tends to perform better as the population number increases, which suggests that the dimension of the solution space is too large for the current population. Optimizing the parameters of the GA could improve its performance. Nonetheless, the parameter configurations of GWO and MGWO are much simpler. They enjoy superior applicability to diverse problems [12], which is preferred in practical applications.

To further compare the modified and original GWO, Opt II was selected in the next experiment. Twenty independent tests were conducted. This time, the two optimizers were both allowed to stop in advance to save time. The experiment settings and results are presented in Table V. The MGWO still shows a better converging rate, and consumes less time and simulation resources. The average cost values after each iteration are shown in Figure 13(a). If the optimizer stopped in advance, the cost values in the subsequent iterations were set to -22.5, the lower bound of the obtained data. It is observed that the MGWO minimizes the cost value more effectively. In Figure 4(b), the average iteration number needed to obtain a certain cost value is calculated through linear interpolation. The MGWO requires fewer iterations when the objective cost value is below -10. Since one iteration represents 30 simulation runs in Opt II, the MGWO significantly reduces the time cost of the design procedure.

Table V

Optimizer Settings		
	GWO	MGWO
Population	20	
Max iteration number	30	
Converging criterion	Cost value <-20	
Results		
Iteration required on average	26.5	23.375
Converging rate	60%	80%
Worst final cost	-15.7	-19.1

The proposed antenna structure seen in Figure 14 and the optimization algorithm are verified. Two 3DP-friendly integrated horn antennas, H1 and H2, were designed based on the MGWO. Initially, the configuration of a wideband corrugated horn antenna was automatically generated based on Table I and II through the optimizer. Then, two OMTs having different operating bands were devised in the same way. The orthogonal ports of H1 operate in different bands for Ku-band satellite communication. The uplink and downlink bands are chosen as the well-known 14/12GHz ones in Asia-Pacific. To further test the flexibility of the optimizer, the second OMT is aimed to cover a wide band.

The configurations of the two integrated horn antennas are presented in Table V and Figure 1. As presented in Figure 14, the two antennas are printed holistically by an EOS M 290 3D printer with aluminum alloy powder through direct metal laser sintering without redundant supports. No assembling process or fixtures are required, either. Consequently, the weight of these antennas is around 200g each. The thickness of the antenna walls is beyond 1.5 mm to ensure structural robustness. Their ports are connected to BJ120 (WR-75/WG-17) waveguide-coaxial adaptors with standard flanges.

Table VI
ANTENNA CONFIGURATIONS CORRESPONDING TO FIGURE 1

Wideband corrugated horn for H1 and H2							
φ_h	34.2 deg	d_3	3 mm	d_7	3.4 mm	l_2	6.4 mm
r_{cwg}	9 mm	d_4	3.7 mm	d_8	2.1 mm	l_3	7.6 mm
d_1	6.4 mm	d_5	3 mm	d_9	3.61 mm	l_4	8.6 mm
d_2	2 mm	d_6	1.5 mm	l_1	5.6 mm		
Dual-band OMT for H1				Wideband OMT for H2			
c_0	1.5 mm	b_3	6.8 mm	c_0	7.4 mm	b_3	6.85 mm
a_1	16.7 mm	b_4	6.8 mm	a_1	16.45 mm	b_4	6.85 mm
a_2	18 mm	c_1	15 mm	a_2	18 mm	c_1	10 mm
a_3	12.4 mm	c_2	5.4 mm	a_3	19.05 mm	c_2	7.2 mm
a_4	19.05 mm	c_3	9.8 mm	a_4	19.05 mm	c_3	2.1 mm
b_1	4.5 mm	c_4	2.4 mm	b_1	7 mm	c_4	3.2 mm
b_2	6.8 mm			b_2	4.6 mm		

The measured and simulated S parameters show good agreement, as presented in Figure 15. H1 operates in 12.25-12.75 GHz and 14-14.5 GHz with Port 1 and Port 2 excited, respectively. As for H2, the overlapped operating band of the two ports is 10.8-14.7 GHz. Since the corrugated horn is shared by the two designs, the radiated patterns of H1 are displayed. As presented in Figure 16, fine consistency is observed between the measured and simulated main beams. Beam equalization and stability are attained. However, the measured cross-polarization is not reasonable, which is because the maximum transmitted power of the far-field measurement system is not enough for the Ku band.

It will be appreciated that many further modifications and permutations of various aspects of the described embodiments are possible. Accordingly, the described aspects are intended to embrace all such alterations, modifications, and variations that fall within the spirit and scope of the appended claims.

Throughout this specification and the claims which follow, unless the context requires otherwise, the word “comprise”, and variations such as “comprises” and “comprising”, will be understood to imply the inclusion of a stated integer or step or group of integers or steps but not the exclusion of any other integer or step or group of integers or steps.

The reference in this specification to any prior publication (or information derived from it), or to any matter which is known, is not, and should not be taken as an acknowledgment or admission or any form of suggestion that that prior publication (or information derived from it) or known matter forms part of the common general knowledge in the field of endeavour to which this specification relates.

Claims

1. A unitary device comprising:

a horn antenna disposed about a horn axis and having an engineered inner surface; and

an integrated orthomode transducer comprising a waveguide transition and at least two separate waveguides each having an internal surface, the waveguide transition connecting the at least two separate waveguides to the antenna, wherein the orthogonal transducer is adapted to couple at least two orthogonal linear polarized fields from the at least two separate waveguides into the waveguide transition for transmission by the antenna, and/or decouple at least two orthogonal linear polarized fields received by the waveguide transition from the antenna into respective ones of the at least two separate waveguides.

2. The unitary device according to claim 1, wherein the inner surface of the horn antenna is designed according to a broad class of optimisation algorithms.

3. The unitary device according to any one of claims 1 to 2, wherein the internal surface of at least one of the at least two separate waveguides is designed according to a broad class of optimisation algorithms.

4. The unitary device according to any one of claims 1 to 3, wherein the horn antenna has a circular cross-section.

5. The unitary device according to any one of claims 1 to 4, wherein the horn antenna has a square cross-section.

6. The unitary device according to any one of claims 1 to 5, wherein the horn antenna is adapted to support two or more waveguide modes corresponding to the at least two orthogonal linear polarized fields.

7. The unitary device according to any one of claims 1 to 6, wherein the horn antenna operates in 12.25-12.75 GHz and 14-14.5 GHz.

8. The unitary device according to any one of claims 1 to 7, wherein the waveguide transition is a quasi-elliptical waveguide transition connecting a rectangular and a circular waveguide.

9. The unitary device according to any one of claims 1 to 8, wherein the inner surface of the horn antenna comprises a plurality of ridges, each ridge having a horizontal ridge width, being oriented parallel to the horn axis, with the ridge being located at slots along the inner surface of the horn antenna, each slot having a vertical slot height, and a horizontal slot width, being oriented parallel to the horn axis.

10. The unitary device according to any one of claims 1 to 9, wherein the horn antenna has a flare angle being the angle between a line drawn parallel to the horn axis and a line passing through a top surface of adjacent ones of said ridges.

11. The unitary device according to any one of claims 1 to 10 is formed from at least one of a metal material and a plastic material.

12. The unitary device according to any one of claims 1 to 11, wherein the waveguide transition tapers away from the horn antenna.

13. The unitary device according to any one of claims 1 to 12, wherein the at least one of the at least two of the separate waveguides has a rectangular cross-section.

14. The unitary device according to any one of claims 1 to 13, wherein the at least one of the at least two of the separate waveguides has a circular cross-section.

15. The unitary device according to any one of claims 1 to 14, wherein the at least one of the at least two of the separate waveguides has a waveguide axis at a non-zero angle to the horn axis.

16. The unitary device according to any one of claims 1 to 15, wherein a length of the at least one of the at least two of the separate waveguides is formed from a sequence of sections, each section having a length, width and height, and varying from each adjacent said section in the sequence, in at least one of the length, width and height.

17. An antenna assembly, comprising:

a unitary device according to any one of claims 1 to 16;

a perforated reflector; and

a platform for stabilizing the utility device and the perforated reflector, wherein the horn antenna of the unitary device functions as the feed for the perforated reflector, and a phase center of the horn antenna of the unitary device is at a focus of the perforated reflector.

18. A manufacturing method for manufacturing the antenna assembly according to claim 17, comprising manufacturing at least one of the unitary device, the perforated reflector, and the platform using three-dimensional printing technology.

19. A manufacturing method for manufacturing the unitary device according to any one of claims 1 to 16, comprising manufacturing the unitary device in at least two separate blocks.

20. The manufacturing method according to claim 19 further comprises at least one of:

manufacturing each part of the at least two separate blocks as one or more of external protrusions, holes and partially holes; and providing alignment pins and threaded holes on the at least two separate blocks to facilitate assembly.

21. A method of designing the horn antenna or the separate waveguides of the orthomode transducer based on grey wolf optimizer, comprising:

generating initialization population in a pre-defined solution space;

calculating a fitness value of each grey wolf in the initialization population according to a pre-defined fitness function, each grey wolf defining a solution at a position in the solution space; and

repeatedly:

selecting a predetermined number of fitness values based on an ordering of fitness values from large to small ("**best fitness values**"), and identifying and storing as X_α, X_β, and X_δ a position of each best fitness value based on the respective grey wolf;

updating and storing position for each grey wolf according to one or more pre-defined functions; and

updating and storing the fitness value of each grey wolf in each updated position according to the pre-defined fitness function; and

outputting X_α when a predetermined maximum number of repetitions is reached.

22. The method of claim 21, wherein, for each repetition of updating a position for each grey wolf, the method further comprises comparing the updated position with each position of a previous repetition, to determine whether or not to update the fitness value with the updated position.

23. The method of claim 21, wherein the fitness function for designing the horn antenna according to any one of 1 to 7 is determined according to:

$$F_{horn} = B_1 f_{S_{11}} + B_2 f_{Beam} + B_3 f_{XP} + B_4 f_{Size}, \text{ where } \sum_n B_n = 1$$

$$f_{S_{11}} = \sum_{m=1}^{2} u(S_{11\_max}(m) + 20)(S_{11\_max}(m) + 20)^2$$

$$f_{Beam} = \sum_{i=1}^{3} (\max_{j=1,2,3} |BW_{12dB}(i,j) - 63|)^2$$

$$f_{XP} = \sum_{i=1}^{2} u(\max_{j=1,2,3} XPL(i,j) + 30)(\max_{j=1,2,3} XPL(i,j) + 30)^2$$

$$f_{Size} = u(\sum_k d_k - d_{total})(\sum_k d_k - d_{total})^2$$

in which B_i (i=14) is the positive weighted coefficient indicating the importance of each requirement, $u(x)$ denotes step function, $S_{11\_max}(m)$ is maximum S_{11} parameter in dB in the m-th band, $Bandwidth_{12dB}(i,j)$ and $XPL(i,j)$ are the 12dB beamwidth in degree and cross-polarization level in dB, respectively, in the j-th plane at the i-th frequency, d_k denotes the horizontal ridge width and the horizontal slot width in mm, and d_{total} is size limitation of the horizontal ridge width and the horizontal slot width.

24. The method of claim 21, wherein the fitness function for designing the horn antenna according to any one of 1 to 7 is determined according to:

$$F_{OMT} = D(\sum_n c_n - c_{total})^2 u(\sum_n c_n - c_{total}) + (1-D)(S_{11max} + 20)^2 u(S_{11max} + 20)$$

in which D denotes a positive weighted coefficient, $u(x)$ denotes step function, $S_{11\_max}(i)$ is maximum S_{11} parameter in dB in the operating band, c_n denotes the horizontal interval width for the n^{th} interval.

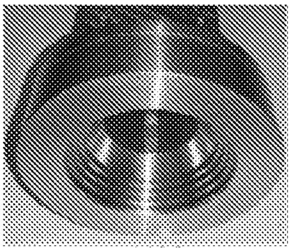

Figure 1(a)

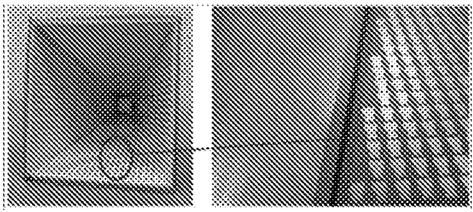

Figure 1(b)

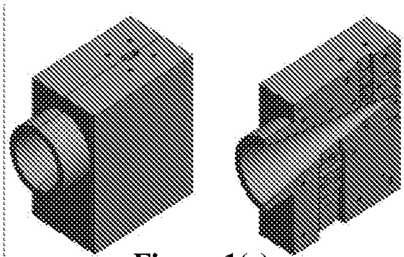

Figure 1(c)

Figure 1

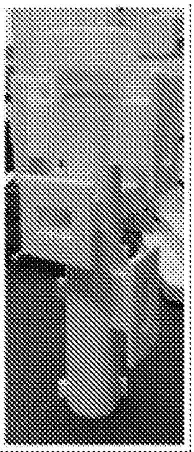

Figure 2(a)

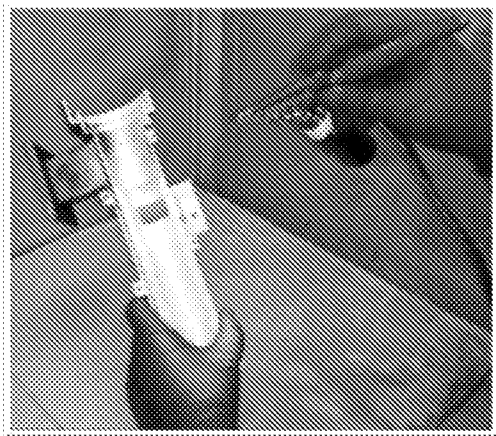

Figure 2(b)

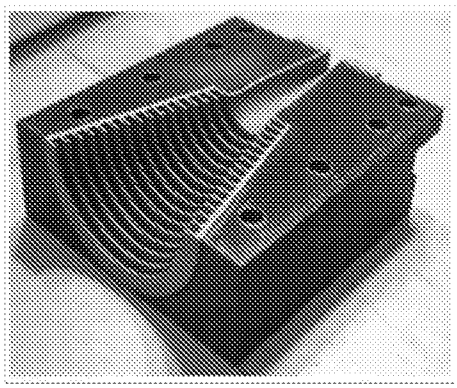

Figure 2(c)

Figure 2

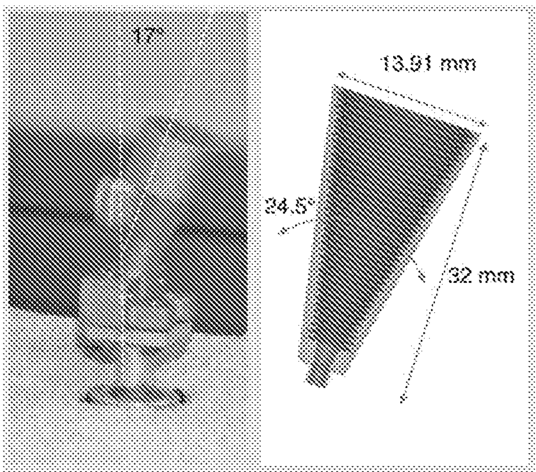

Figure 3(a)

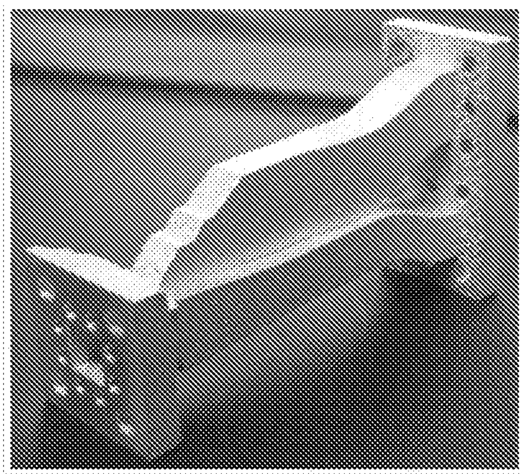

Figure 3(b)

Figure 3

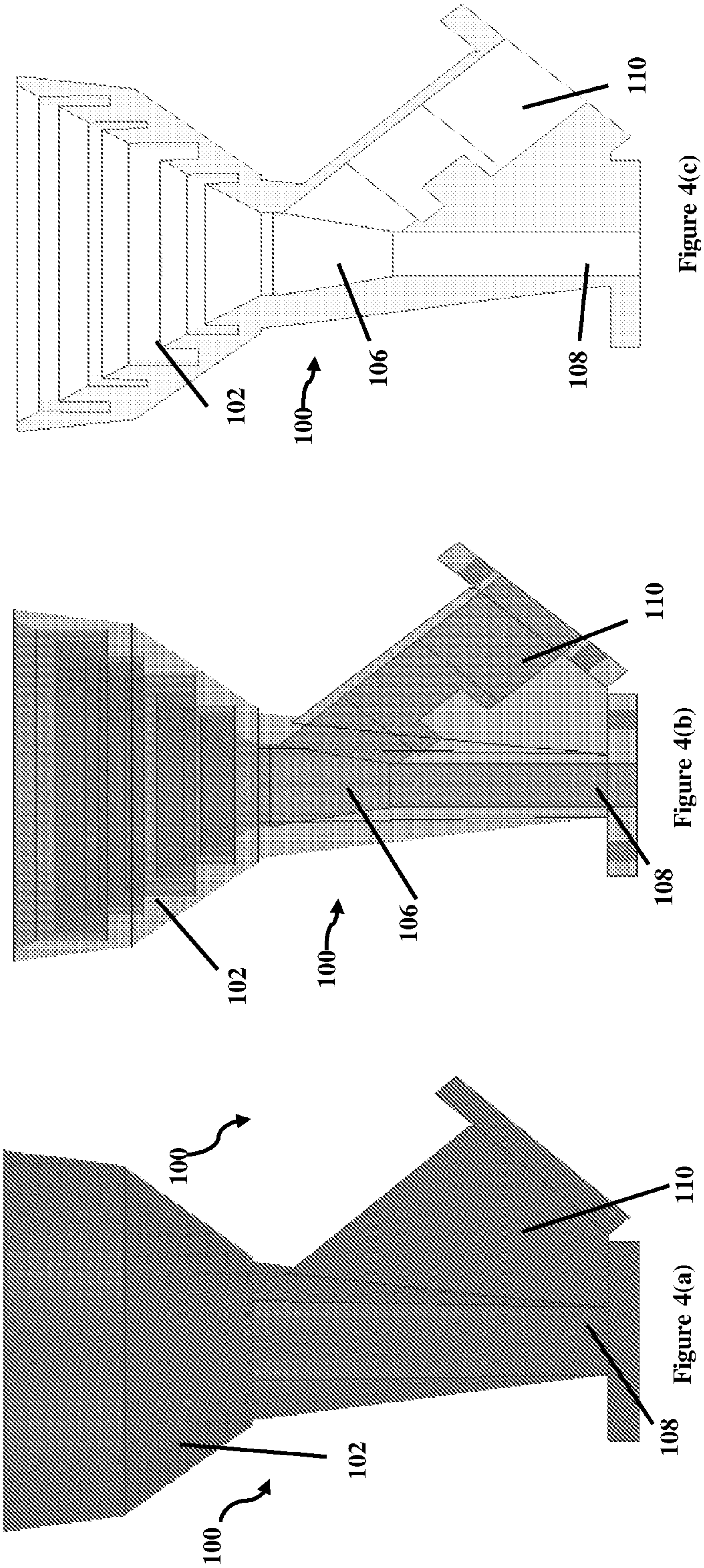

Figure 4(c)

Figure 4(b)

Figure 4(a)

Figure 4

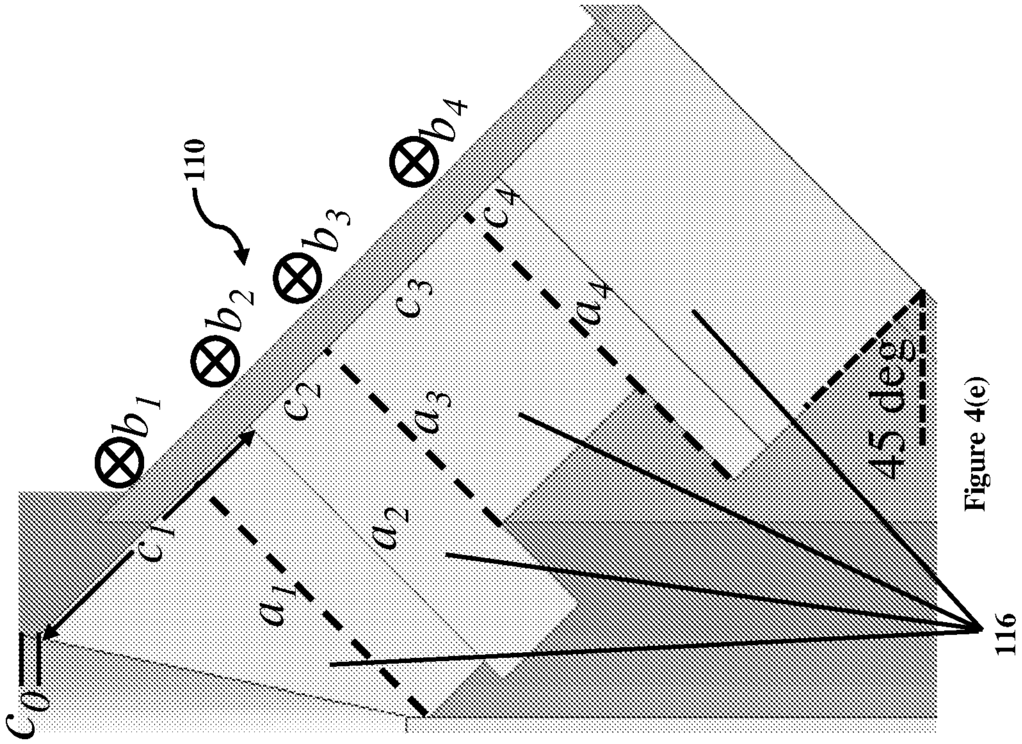

Figure 4(e)

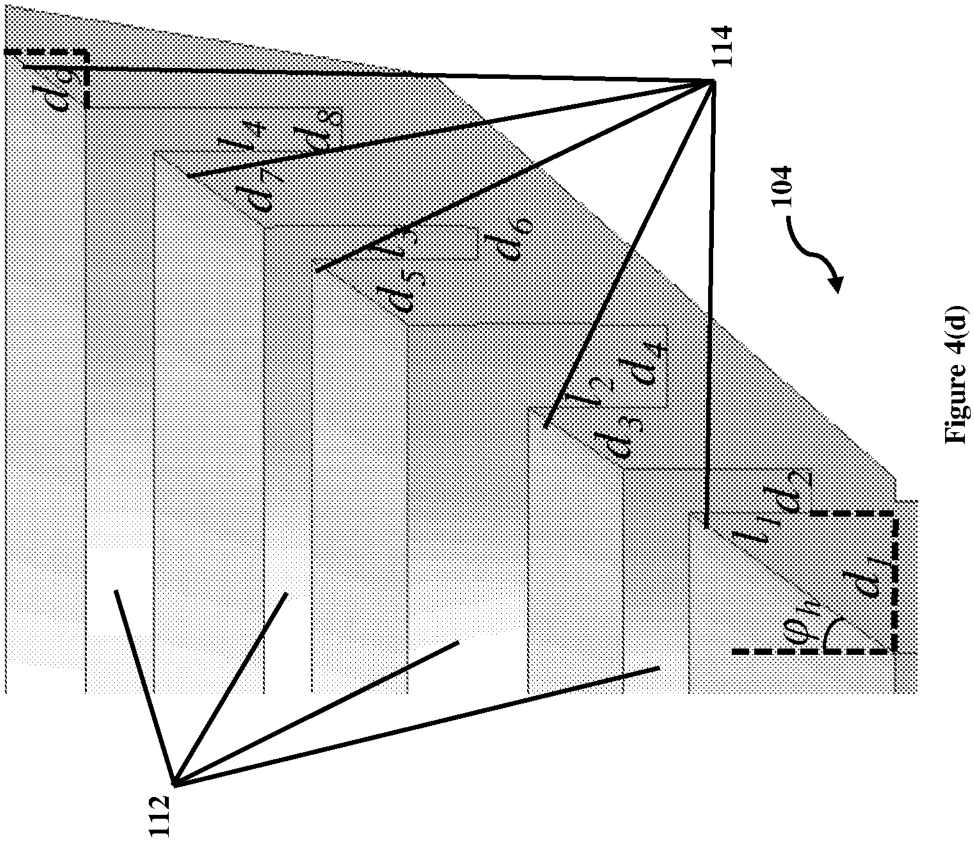

Figure 4(d)

Figure 4

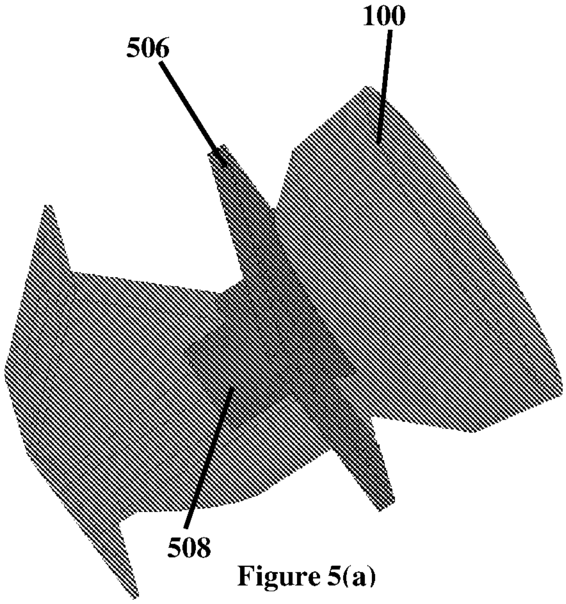

Figure 5(a)

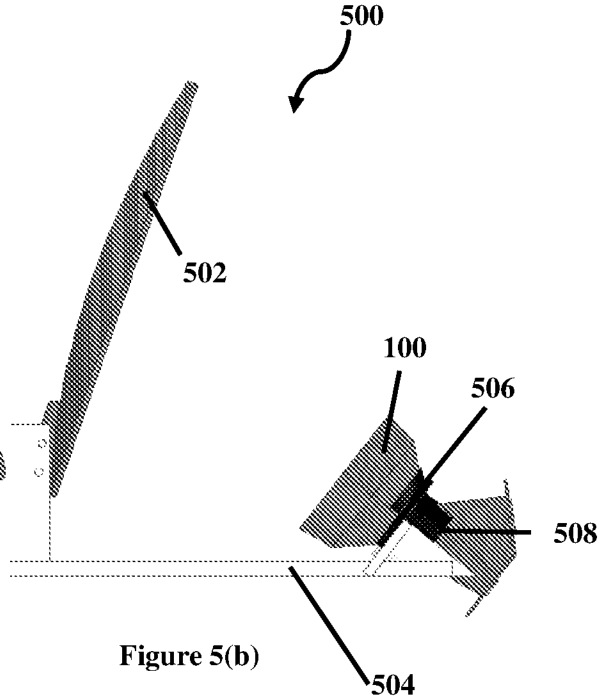

Figure 5(b)

D (mm)	F (mm)	H (mm)	θ_0 (deg)	θ_1 (deg)
230	184	12	38.1	31.5

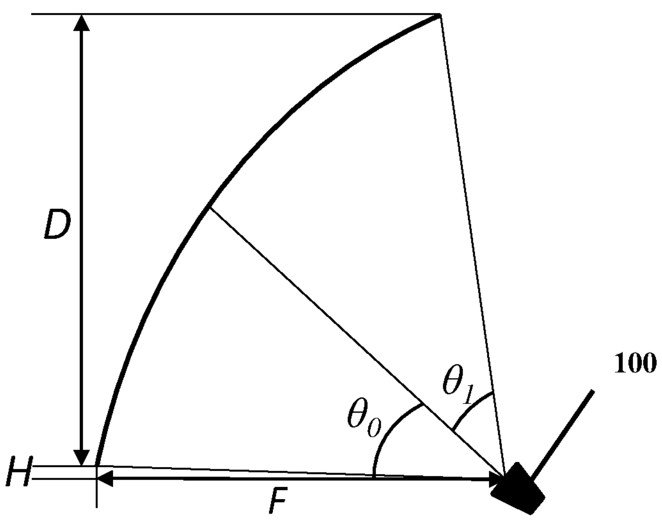

Figure 5(c)

Figure 5

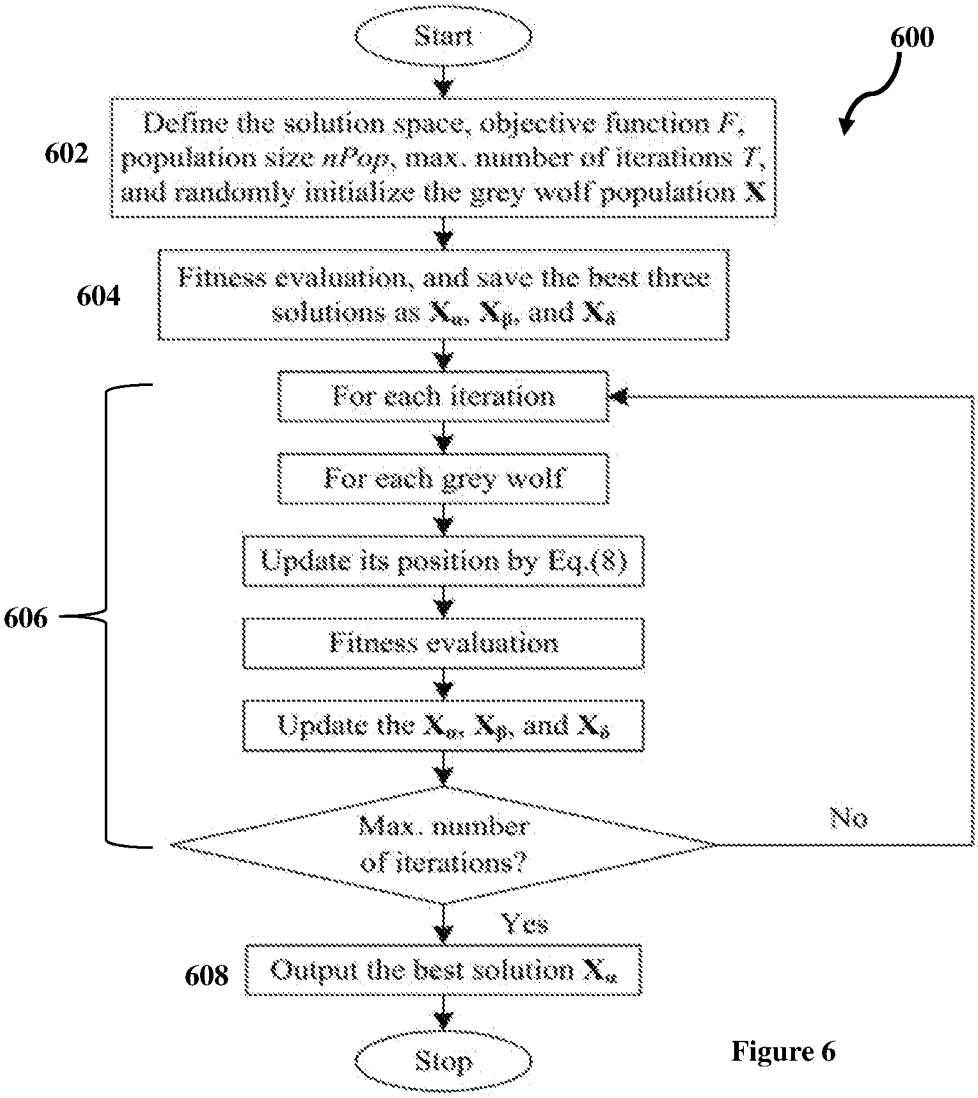

Figure 6

Variables	Lower bound	Upper bound
a_1	5 mm	20 mm
a_2	8 mm	18 mm
a_3	11 mm	20 mm
a_4	14 mm	20 mm
b_1	2 mm	9 mm
b_2	2 mm	9 mm
b_3	2 mm	9 mm
b_4	2 mm	9 mm
c_1	10 mm	25 mm
c_2	2 mm	12 mm
c_3	2 mm	12 mm
c_4	2 mm	12 mm
z	0 mm	8 mm

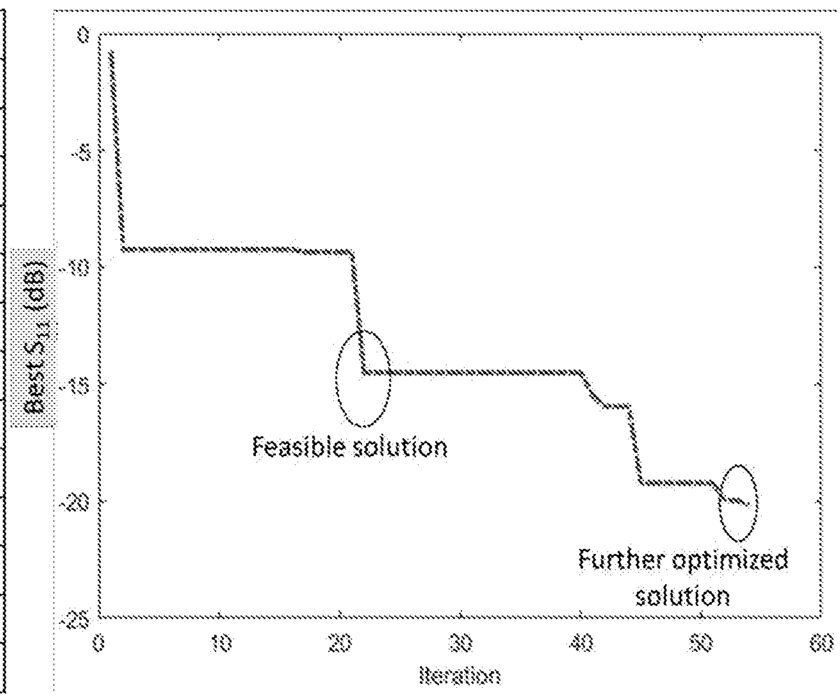

Figure 7

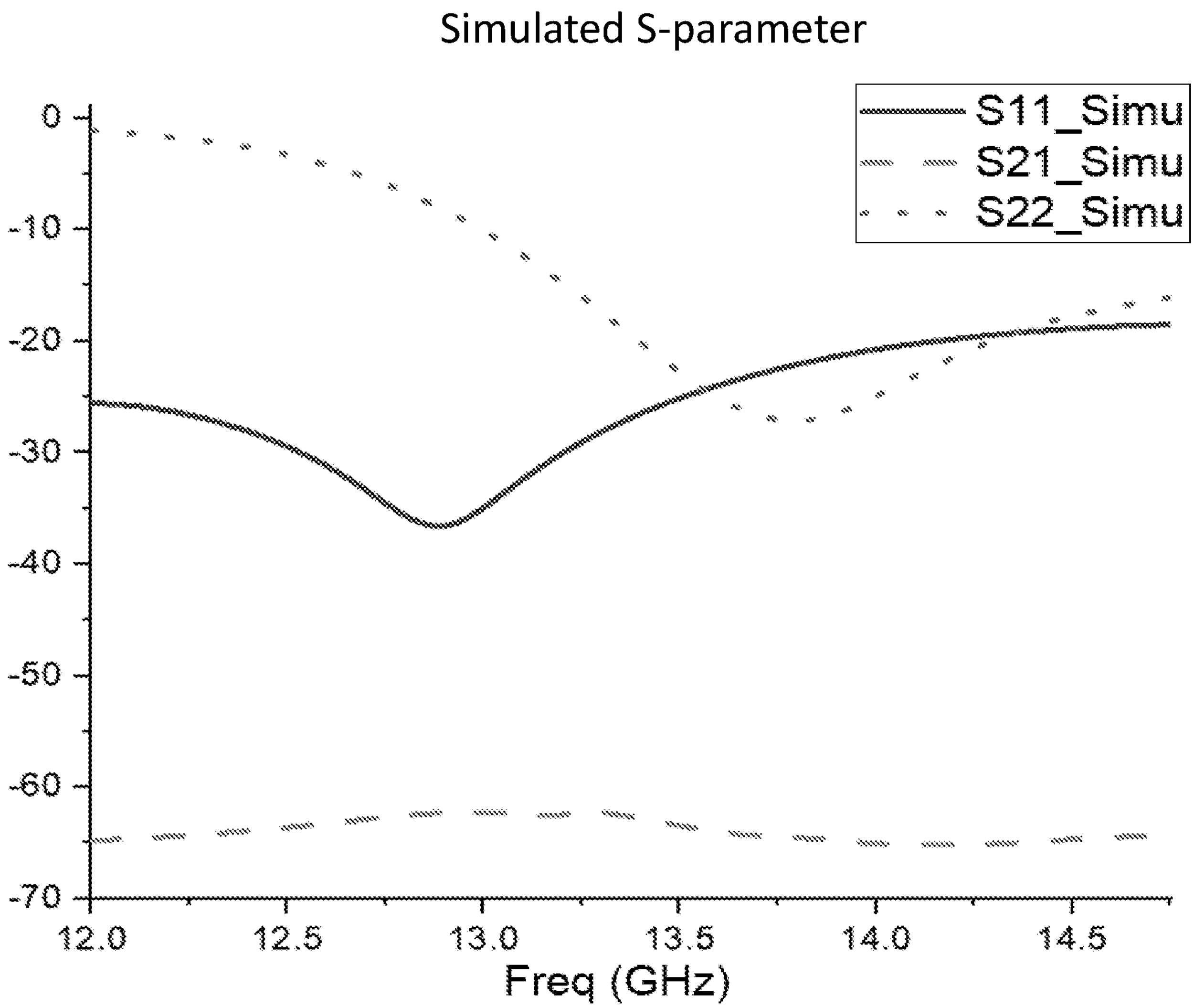

Figure 8(a)

Figure 8

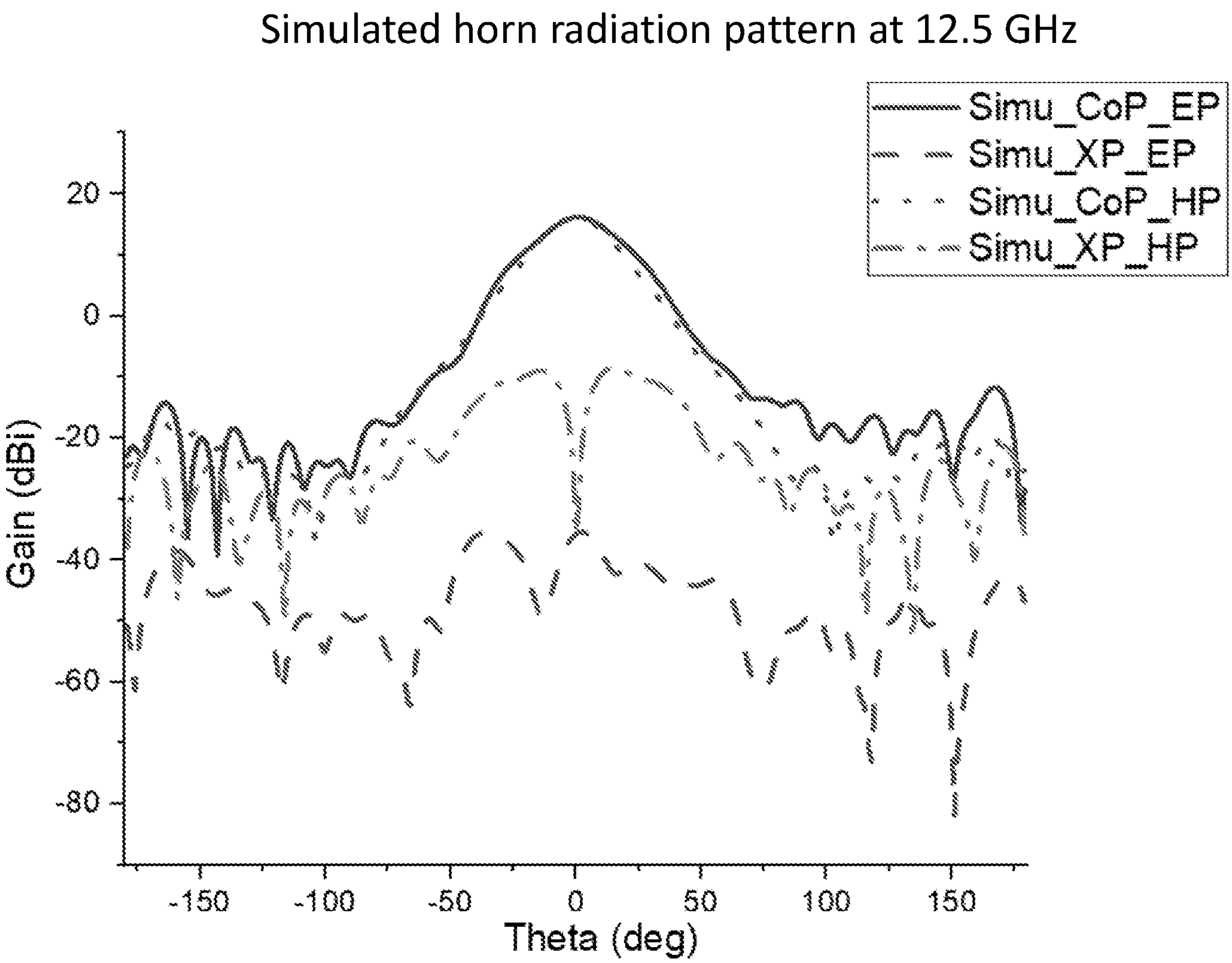

Figure 8(b)

Figure 8

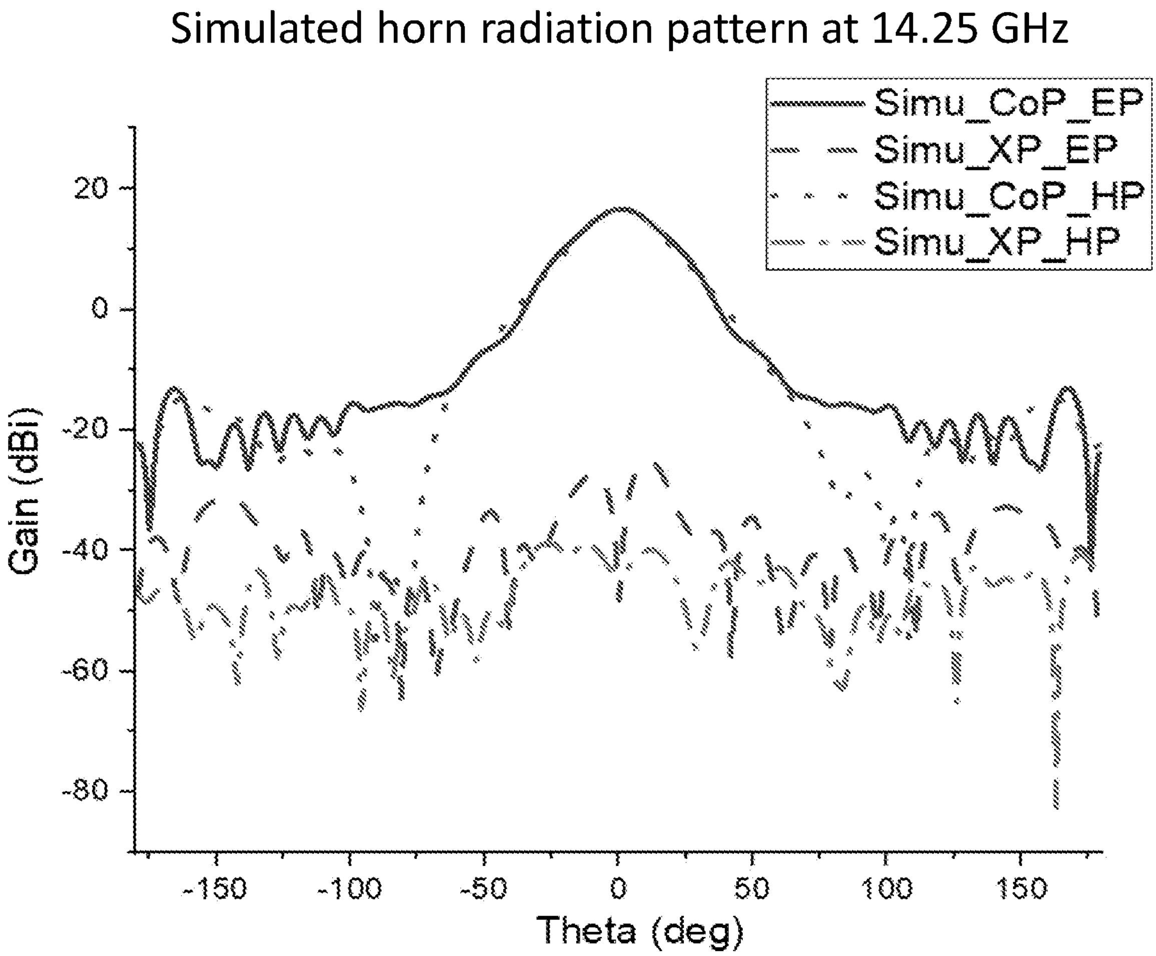

Figure 8(c)

Figure 8

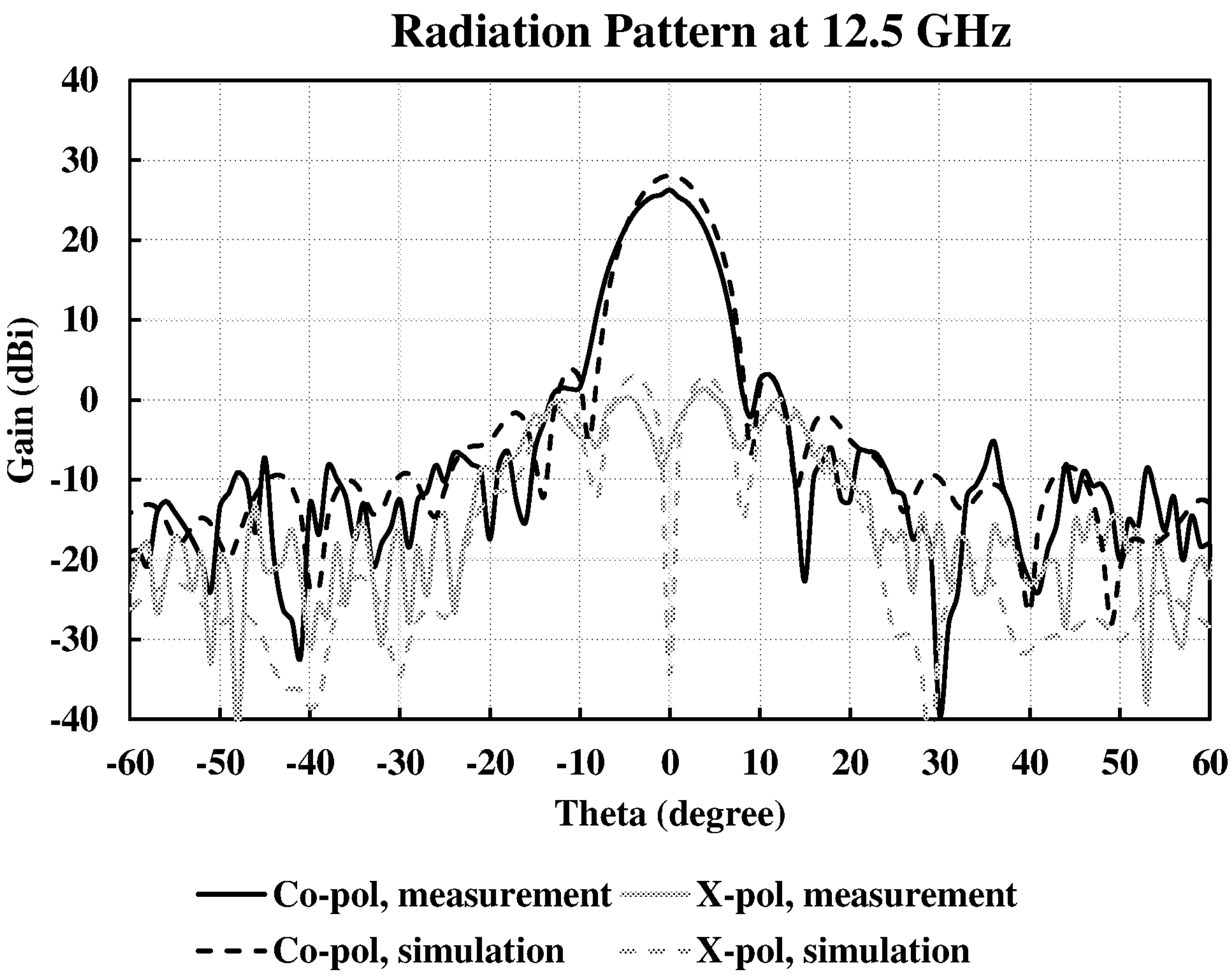

Figure 8(d)

Figure 8

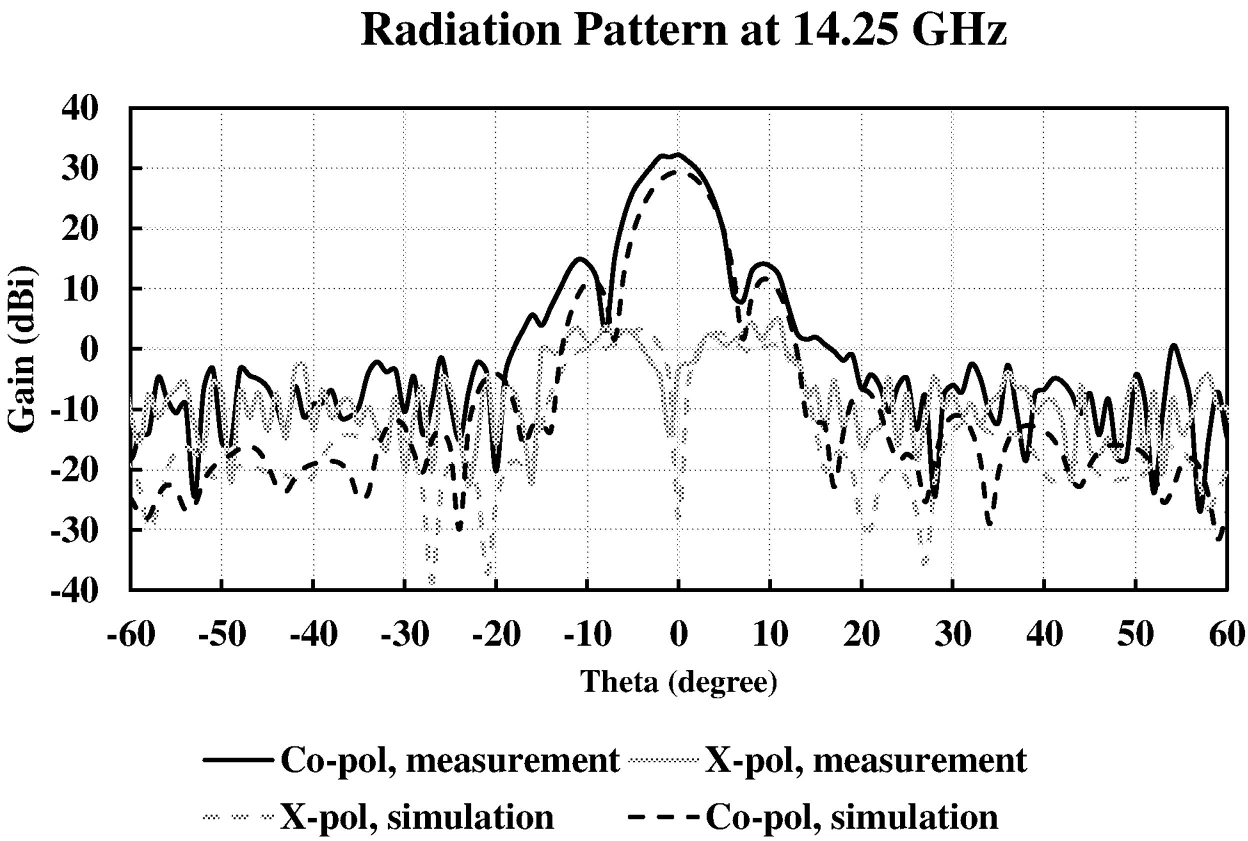

Figure 8(e)

Figure 8

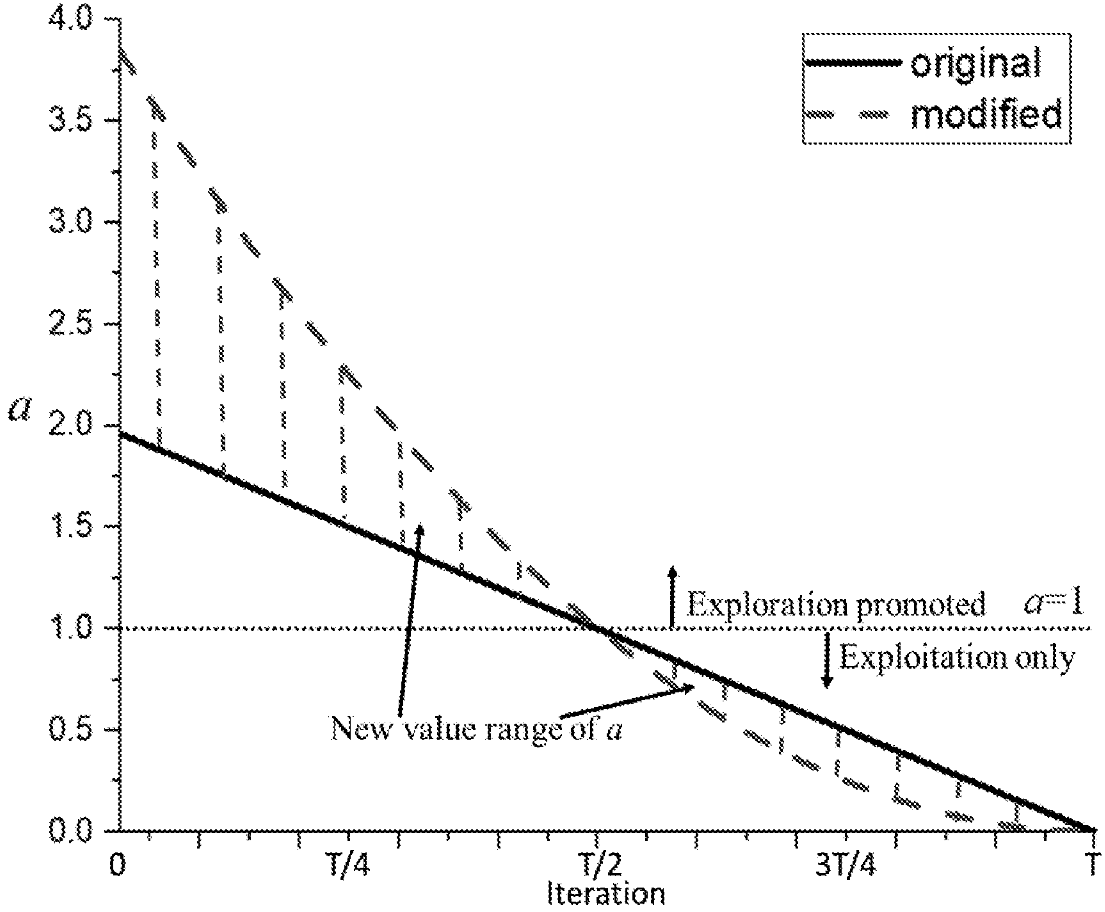
4.0
3.5
3.0
2.5
2.0
1.5
1.0
0.5
0.0
a
original
modified
Exploration promoted
a=1
Exploitation only
New value range of a
0
T/4
T/2
3T/4
T
Iteration

Figure 9

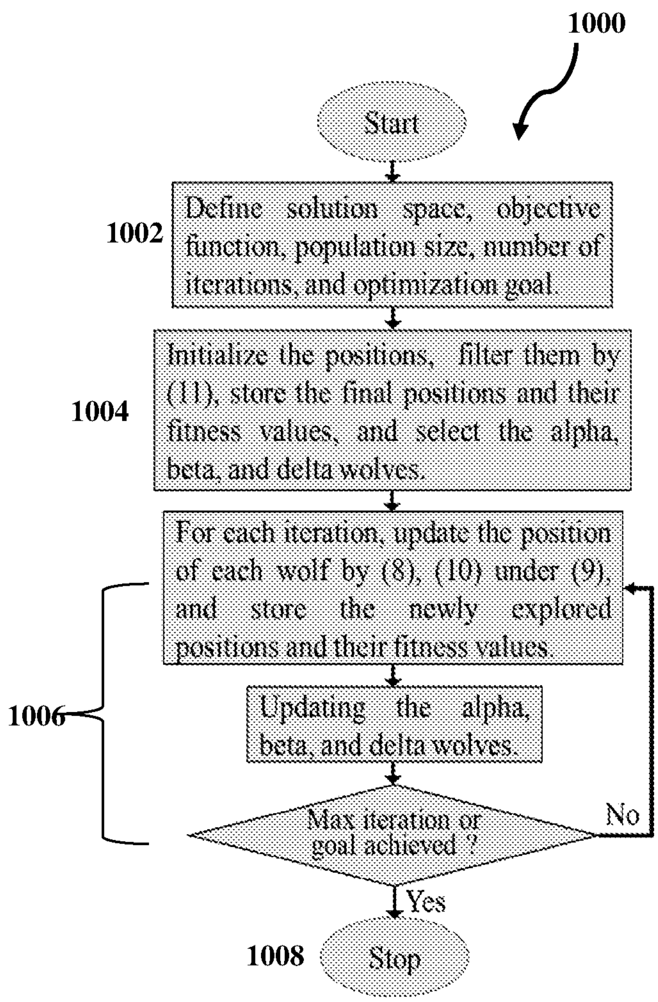
1000
Start
1002
Define solution space, objective function, population size, number of iterations, and optimization goal.
1004
Initialize the positions, filter them by (11), store the final positions and their fitness values, and select the alpha, beta, and delta wolves.
For each iteration, update the position of each wolf by (8), (10) under (9), and store the newly explored positions and their fitness values.
1006
Updating the alpha, beta, and delta wolves.
Max iteration or goal achieved ?
No
Yes
1008
Stop

Figure 10

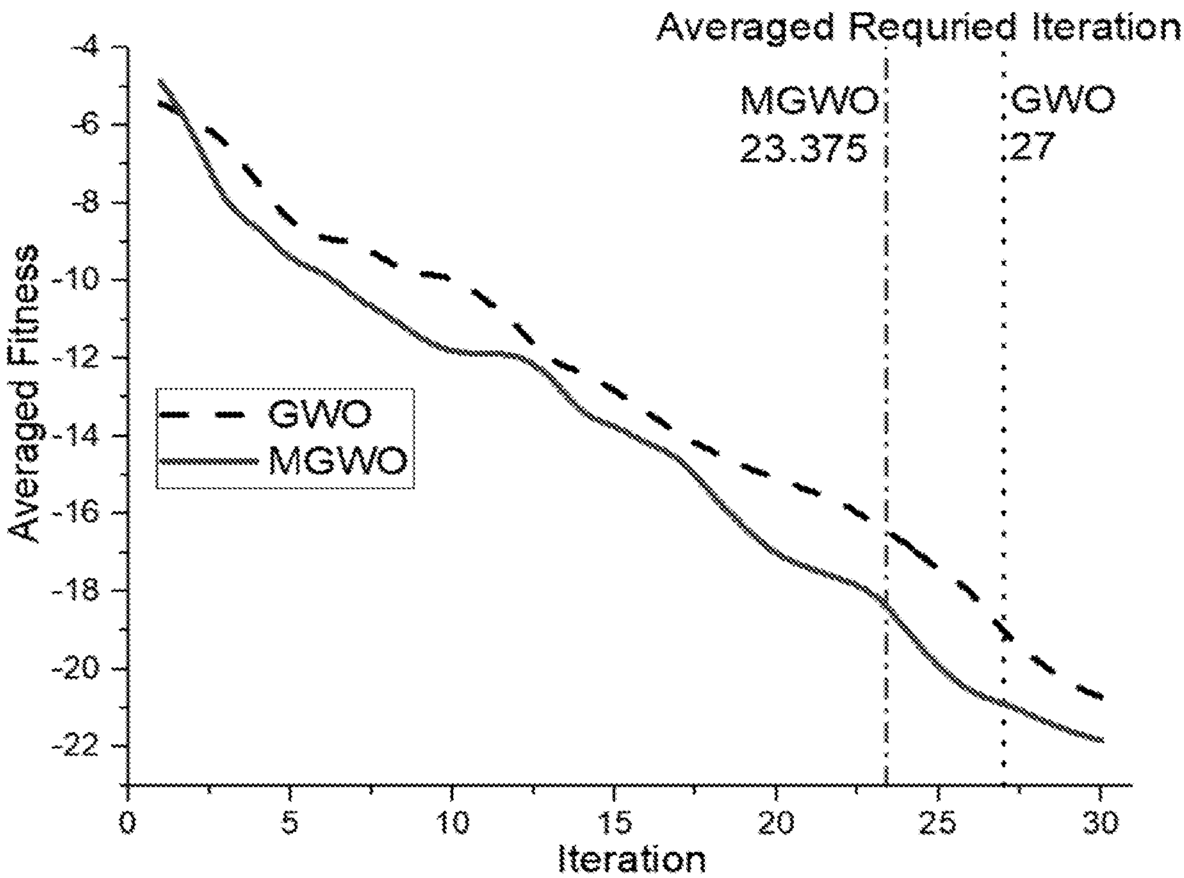
Averaged Requried Iteration
MGWO
23.375
GWO
27
Averaged Fitness
-4
-6
-8
-10
-12
-14
-16
-18
-20
-22
GWO
MGWO
0
5
10
15
20
25
30
Iteration

Figure 11

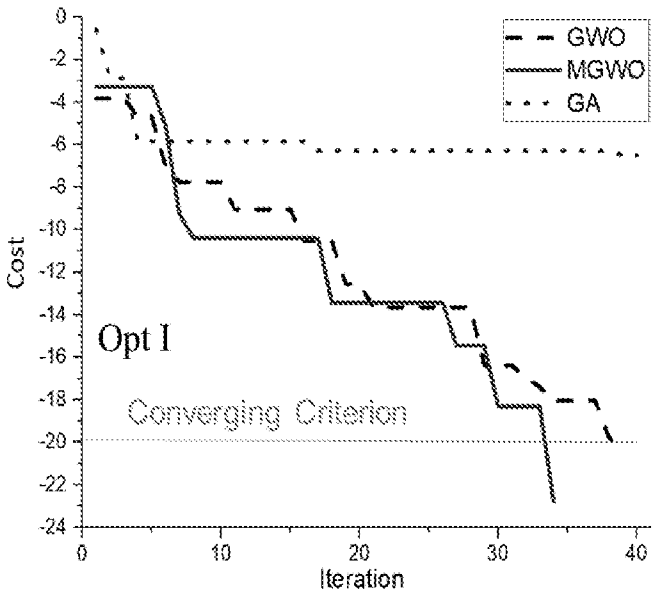

Figure 12(a)

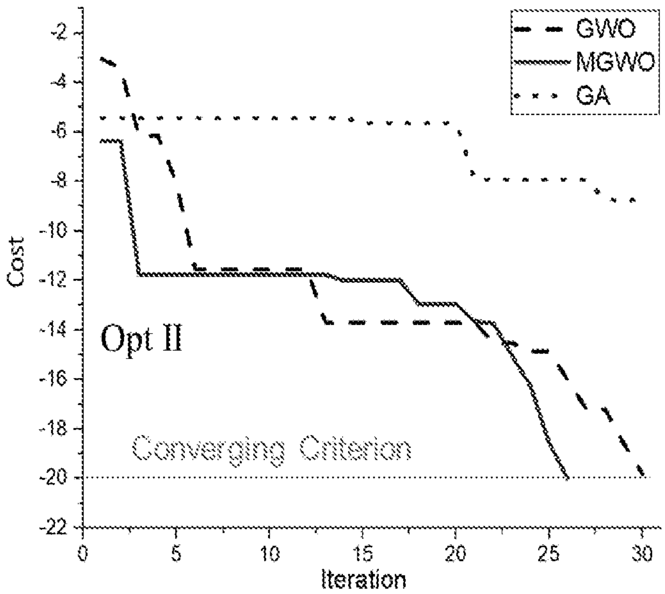

Figure 12(b)

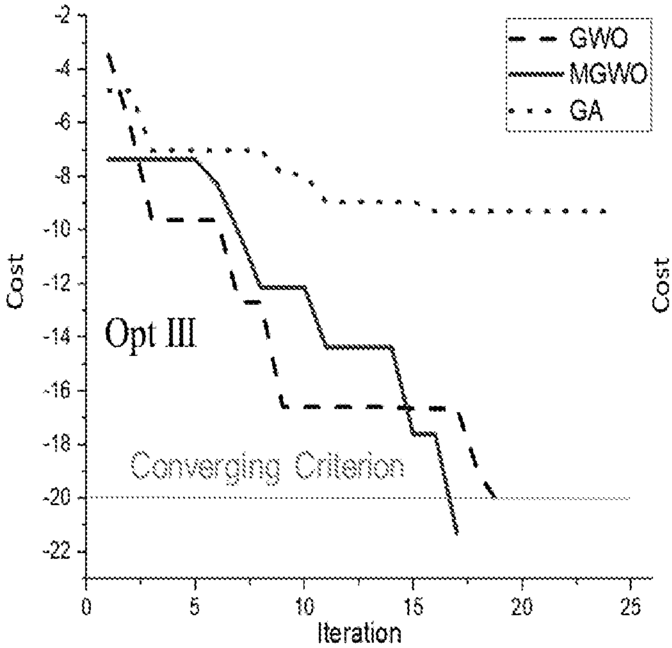

Figure 12(c)

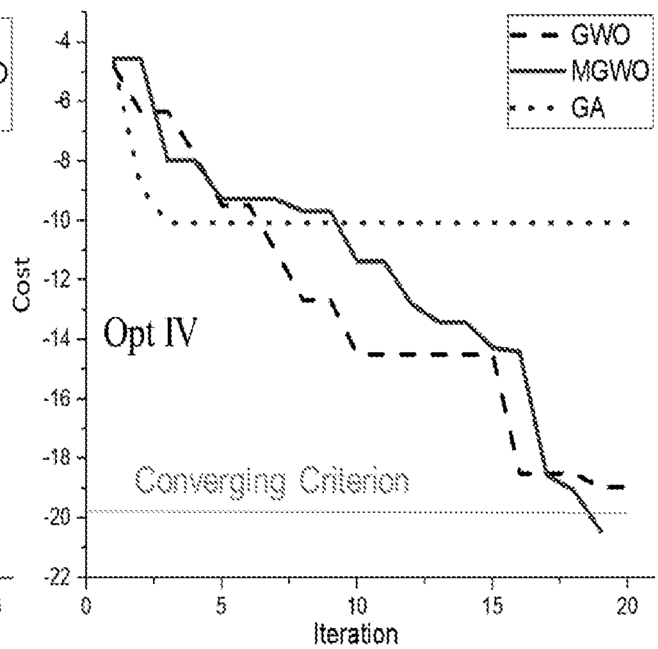

Figure 12(d)

Figure 12

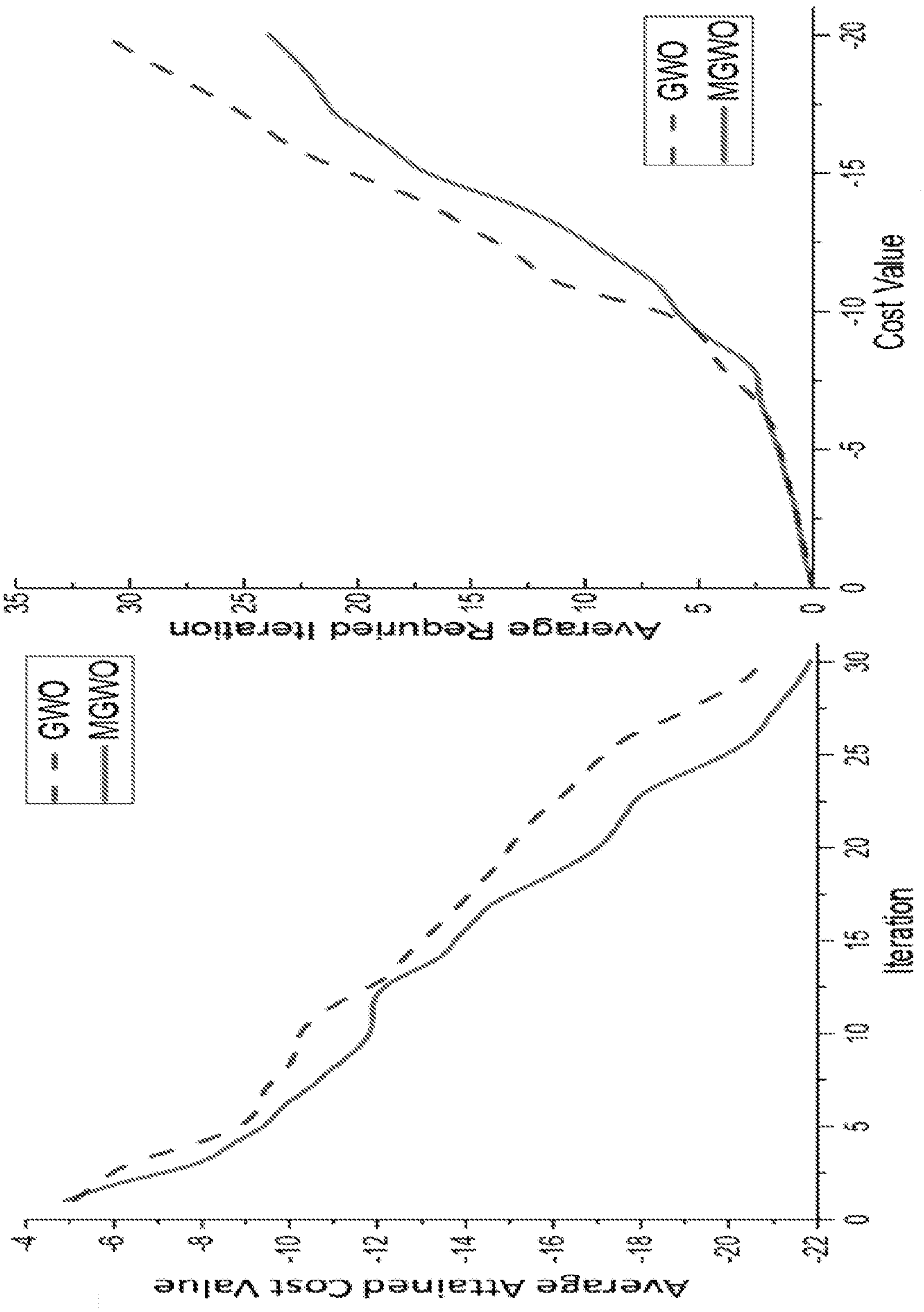

Figure 13(a)

Figure 13(b)

Figure 13

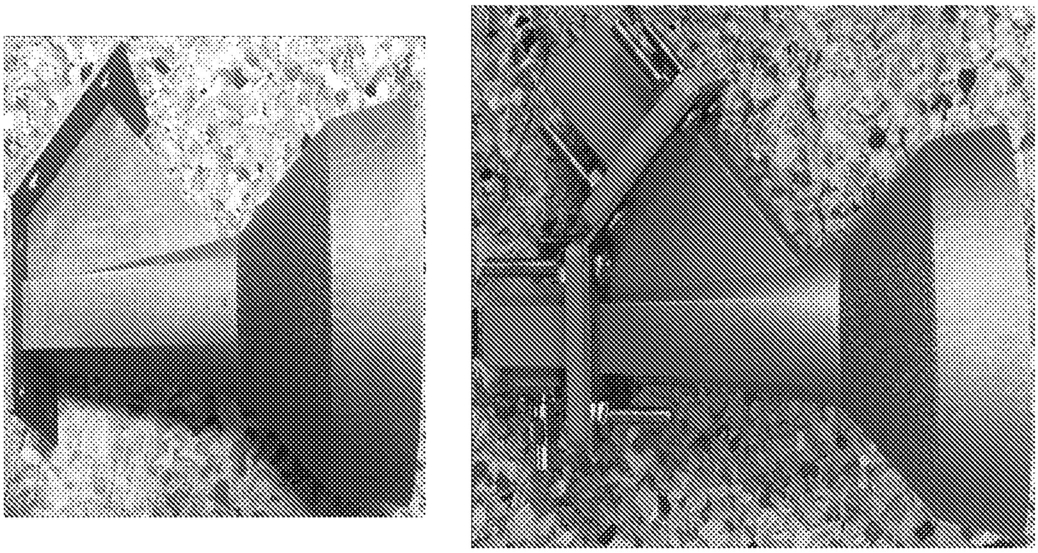

Figure 14

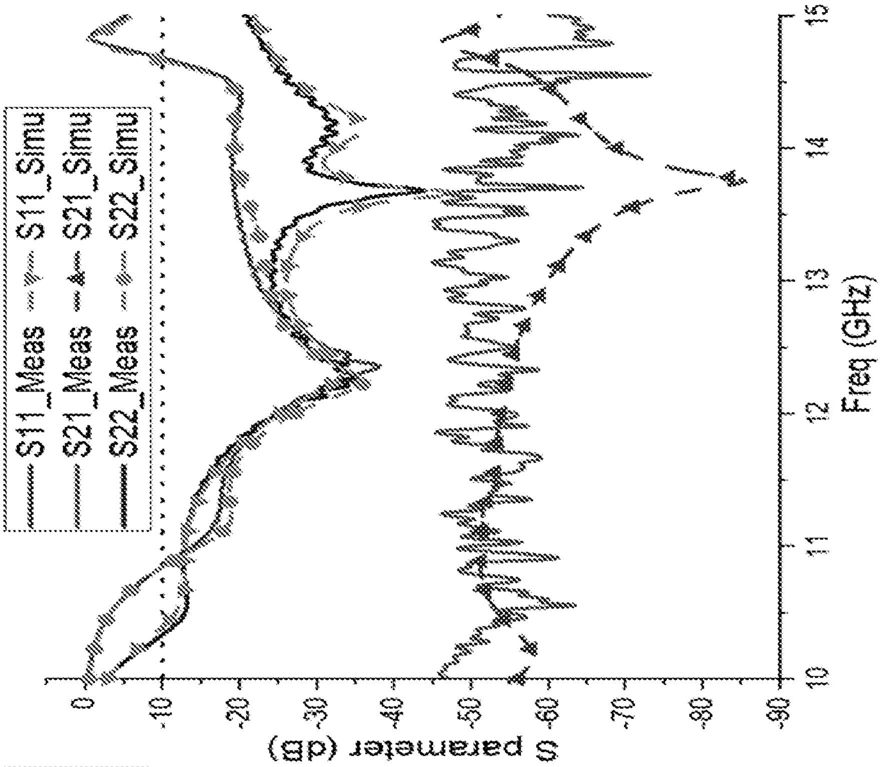

Figure 15(b)

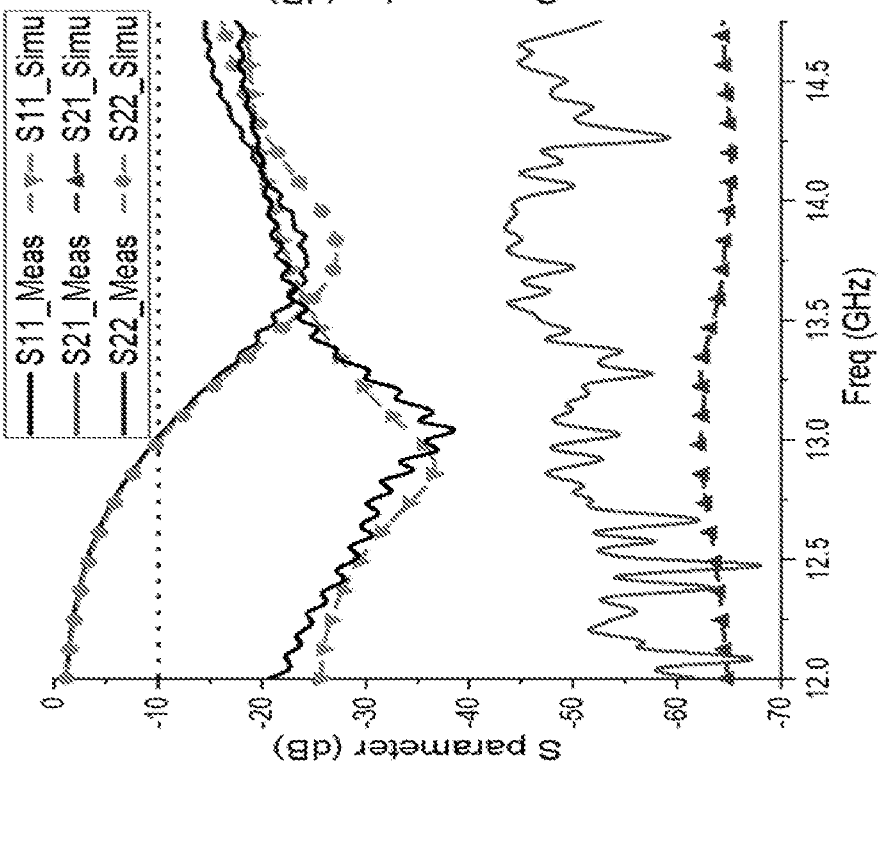

Figure 15(a)

Figure 15

Radiation Pattern at 12.5 GHz

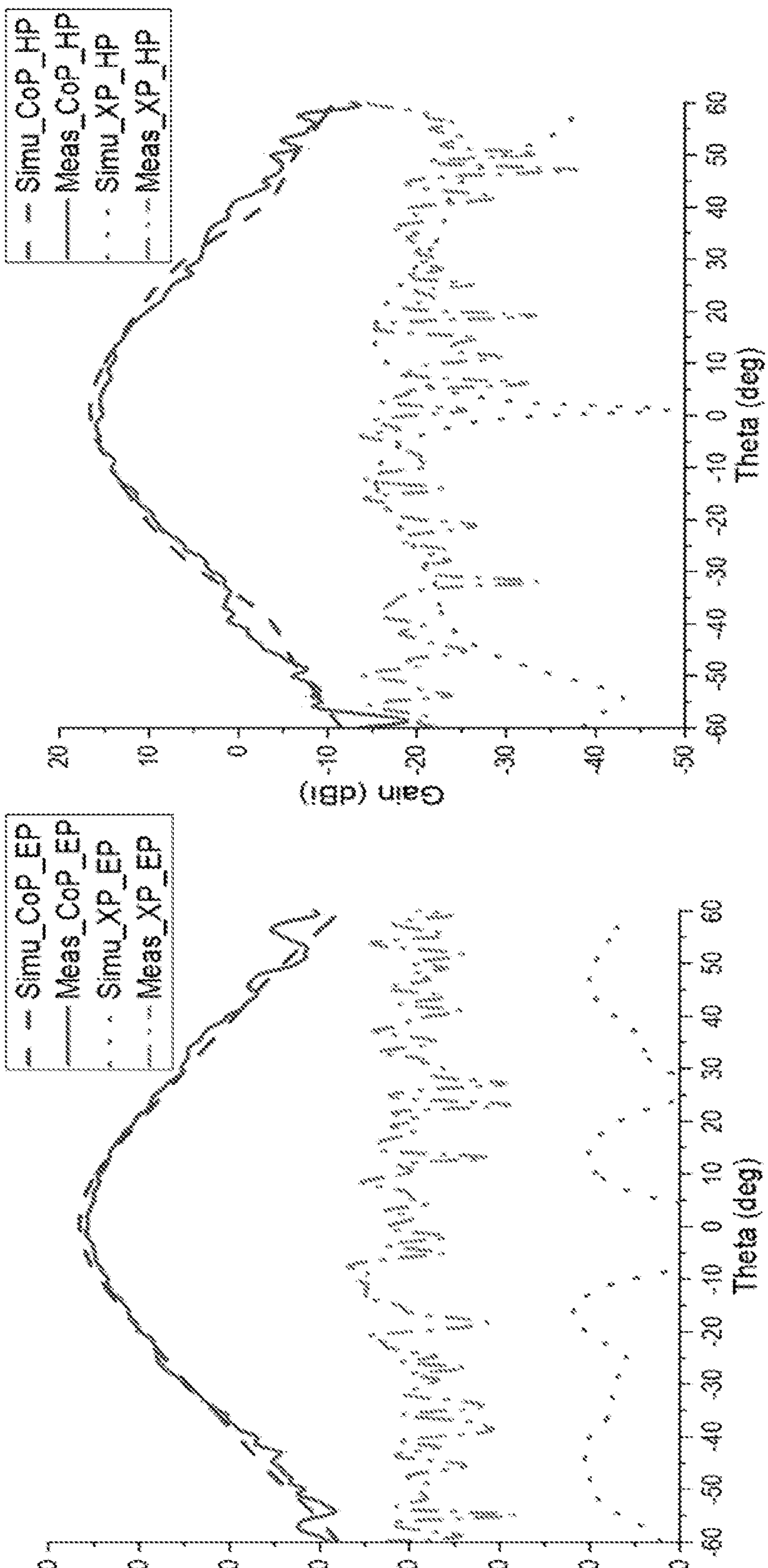

Figure 16(a)

Figure 16(b)

Figure 16

Radiation Pattern at 14.25 GHz

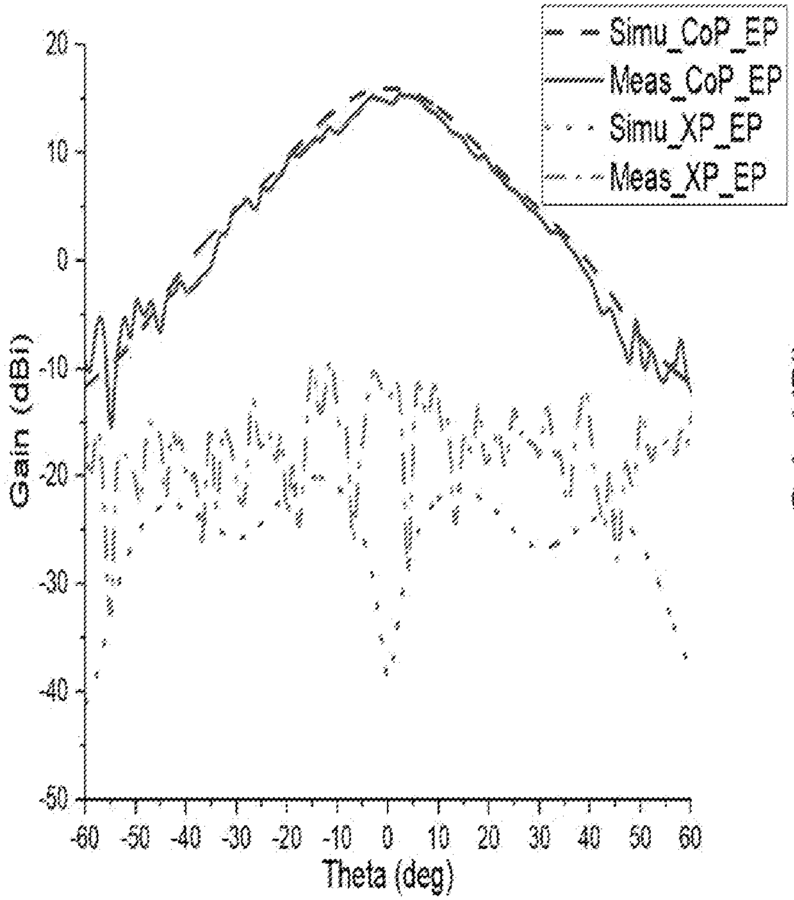

Figure 16(c)

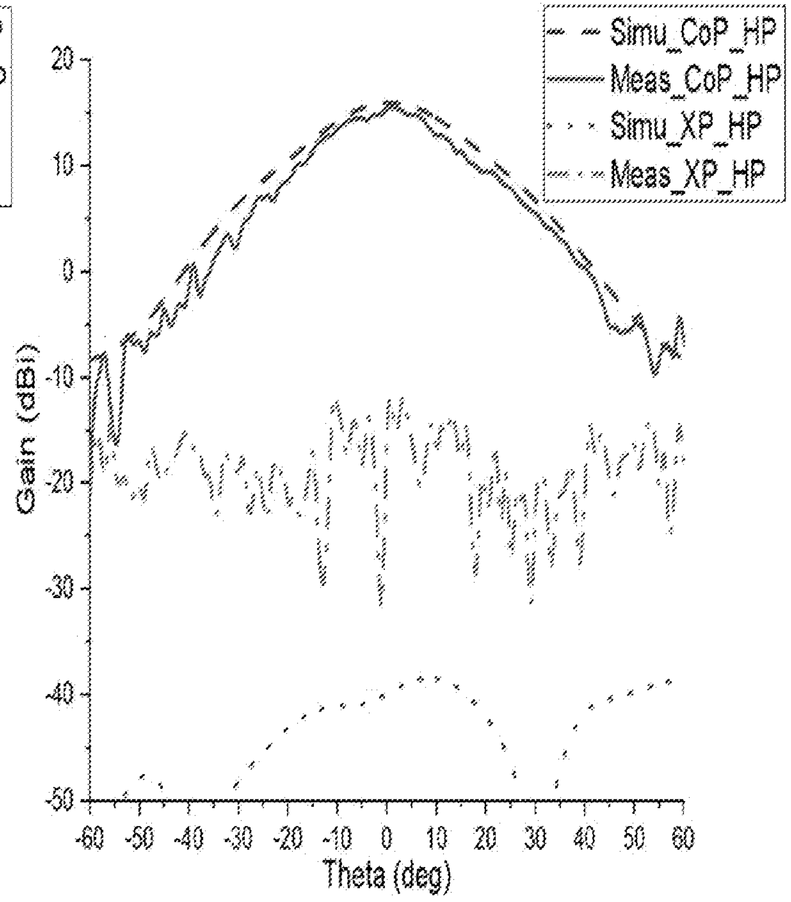

Figure 16(d)

Figure 16

INTERNATIONAL SEARCH REPORT

International application No.
PCT/SG2021/050430

A. CLASSIFICATION OF SUBJECT MATTER

See Supplemental Box

According to International Patent Classification (IPC)

B. FIELDS SEARCHED

Minimum documentation searched (classification system followed by classification symbols)

H01Q, H01P, G06N, B33Y

Documentation searched other than minimum documentation to the extent that such documents are included in the fields searched

Electronic data base consulted during the international search (name of data base and, where practicable, search terms used)

Databases: FAMPAT, CNKI

Keywords: orthomode transducer, horn antenna, unitary, monolithic, 3D printing, additive manufacturing, dual polarization, grey wolf, 正交模式变换器, 喇叭天线, 酉, 整体式, 3d 打印, 添加剂制造, 双极化, 灰狼 and other related terms

C. DOCUMENTS CONSIDERED TO BE RELEVANT

Category*	Citation of document, with indication, where appropriate, of the relevant passages	Relevant to claim No.
X	SAEIDI-MANESH H. ET AL., Design and Fabrication of Orthogonal-Mode Transducer Using 3-D Printing Technology. *IEEE Antennas and Wireless Propagation Letters*, 15 June 2018, Vol. 17, No. 11, pages 2013-2016 [Retrieved on 2021-10-27] <DOI: 10.1109/LAWP.2018.2847654> sections OMT-Horn Antenna Design, Fabrication, table 1, figure 1, 6-9	1-8, 10-20
X	SHEN J. ET AL., Compact W-Band "Swan Neck" Turnstile Junction Orthomode Transducer Implemented by 3-D Printing. *IEEE Transactions on Microwave Theory and Techniques*, 14 May 2020, Vol. 68, No. 8, pages 3408-3417 [Retrieved on 2021-10-27] <DOI: 10.1109/TMTT.2020.2992065> sections OMT Experimental Result, OMT Fabrication, OMT Core Design, figures 1, 1c,1d, 3, 6, 8b, 9	1-7, 9-11, 13-20

☒ Further documents are listed in the continuation of Box C. ☒ See patent family annex.

*Special categories of cited documents:
"A" document defining the general state of the art which is not considered to be of particular relevance
"D" document cited by the applicant in the international application
"E" earlier application or patent but published on or after the international filing date
"L" document which may throw doubts on priority claim(s) or which is cited to establish the publication date of another citation or other special reason (as specified)
"O" document referring to an oral disclosure, use, exhibition or other means
"P" document published prior to the international filing date but later than the priority date claimed
"T" later document published after the international filing date or priority date and not in conflict with the application but cited to understand the principle or theory underlying the invention
"X" document of particular relevance; the claimed invention cannot be considered novel or cannot be considered to involve an inventive step when the document is taken alone
"Y" document of particular relevance; the claimed invention cannot be considered to involve an inventive step when the document is combined with one or more other such documents, such combination being obvious to a person skilled in the art
"&" document member of the same patent family

Date of the actual completion of the international search	Date of mailing of the international search report
27/10/2021 *(day/month/year)*	*01/11/2021* *(day/month/year)*

Name and mailing address of the ISA/SG	Authorized officer
IPOS INTELLECTUAL PROPERTY OFFICE OF SINGAPORE **Intellectual Property Office of Singapore** 1 Paya Lebar Link, #11-03 PLQ 1, Paya Lebar Quarter Singapore 408533	Danny Yap Ming Ann (Mr)
Email: pct@ipos.gov.sg	IPOS Customer Service Tel. No.: (+65) 6339 8616

INTERNATIONAL SEARCH REPORT

International application No.
PCT/SG2021/050430

C (Continuation). DOCUMENTS CONSIDERED TO BE RELEVANT

Category*	Citation of document, with indication, where appropriate, of the relevant passages	Relevant to claim No.
A	CARKACI M.E. ET AL., Design and Prototype Manufacturing of a Feed System for Ku-Band Satellite Communication by using 3D FDM/PLA Printing and Conductive Paint Technology. *International Journal of RF and Microwave Computer-Aided Engineering*, 29 November 2019, pages 1-15 [Retrieved on 2021-10-27] <DOI: 10.1002/MMCE.22062> the whole document especially section Ku-band conical-corrugated horn antenna	
A	BHUTANI A. ET AL., 3D Metal Printed Ku/Ka Band Modified Turnstile Junction Orthomode Transducer. *Proceedings of the Asia-Pacific Microwave Conference 2016*, 9 December 2016, pages 1-4 [Retrieved on 2021-10-27] <DOI: 10.1109/APMC.2016.7931276> the whole document especially figure 6	
A	CN 109755750 A (UNIV BEIHANG) 14 May 2019 the whole document especially figure 3 of the machine translation	

Note: This Annex lists known patent family members relating to the patent documents cited in this International Search Report. This Authority is in no way liable for these particulars which are merely given for the purpose of information.

Patent document cited in search report	Publication date	Patent family member(s)	Publication date
CN 109755750 A	14/05/2019	NONE	

INTERNATIONAL SEARCH REPORT

International application No.
PCT/SG2021/050430

Supplemental Box
(Classification of Subject Matter)

Int. Cl.

H01Q 5/35 (2015.01)

H01P 1/161 (2006.01)

G06N 3/00 (2006.01)

H01Q 13/02 (2006.01)

H01Q 15/00 (2006.01)

H01Q 1/38 (2006.01)

B33Y 80/00 (2015.01)

H01P 3/127 (2006.01)

H01P 3/123 (2006.01)

H01P 11/00 (2006.01)